Sveriges lantbruksuniversitet
Swedish University of Agricultural Sciences

Faculty of Natural Resources and
Agricultural Sciences

Mass Flow and Fate of Per- and Polyfluoroalkyl Substances in a Landfill in Uppsala, Sweden.

Björn Frederik Bonnet

Department of Aquatic Sciences and Assessment
Master thesis • 30 HEC
EnvEuro - European Master in Environmental Science
Uppsala 2017

Mass Flow and Fate of Per- and Polyfluoroalkyl Substances in a Landfill in Uppsala, Sweden.

Björn Frederik Bonnet

Supervisor: Lutz Ahrens

Assistant Supervisor: Hans Christian Bruun Hansen

Examiner: Karin Wiberg

Credits: 30
Level: Advanced level, A2E
Course title: Independent Project in Environmental Science – Master's Thesis
Course code: EX0431
Programme/education: EnvEuro – Master in Environmental Science

Place of publication: Uppsala
Year of publication: 2017
Cover picture:
Title of series:
Part number:
ISSN:
ISBN:
Online publication: http://stud.epsilon.slu.se

Keywords: PFASs, Landfill, Groundwater, Sludge, STP, Mass Flow

Sveriges lantbruksuniversitet
Swedish University of Agricultural Sciences

Faculty of Natural Resources and Agricultural Sciences
Department of Aquatic Sciences and Assessment
Unit/Section (optional)

Abstract

In this study, a landfill has been investigated in terms of the distribution of per- and polyfluoroalkyl substances and the environmental fate. 28 PFASs (13 PFCAs, 4 PFSAs, 3 FOSAs, 2 FOSEs, 3 FOSAAs and 3 FTSAs) have been analysed in 14 leachate, 11 groundwater and 9 sludge samples. Furthermore, 11 samples have been taken in the on-site sewage treatment plant (STP) as well as 12 samples along the receiving water course (total of 57 samples). $\sum$PFAS concentration in the leachate ranged between 59 ng L^{-1} and 1500 ng L^{-1}, in groundwater between 8.5 and 1800 ng L^{-1} and in the sludge between 33 and 438 ng L^{-1}. The composition in the leachate (52%) and the groundwater (60%) was dominated by PFCAs. $C_3 - C_7$ accounted for 98% $\sum$PFCAs in the leachate and 99% $\sum$PFCAs in the groundwater. Sludge samples ranged from 33 ng L^{-1} to 440 ng L^{-1} and were dominated by precursor compounds (FTSAs 37%, PFSAs 33% and PFCAs 7.6% $\sum$PFASs). Long chain PFCAs ($C_8 - C_{14}, C_{16}$) showed detection frequencies of 100% (4.8% $\sum$PFASs (C_{18} included)). PFOS was most abundant in the sludge (30% $\sum$PFASs, 91% $\sum$PFSAs). The STP showed a $\sum$PFASs removal efficiency of 47%, showing highest efficiency for long-chain compounds (88% PFNA, 100% PFDA, 90% PFOS linear and 84% PFOS branched) and precursors (100% for 8:2 FTSA, Me-FOSAA, Et-FOSAA). The total mass flow of PFASs exiting the landfill was estimated with 220 mg g^{-1}. The mass flow in the river showed no long-range effect (30 km) of the landfill concerning the PFASs contamination of surface waters. Conclusively it seems likely that PFASs from the landfill are rather threatening the local groundwater.

Contents

List of Tables

List of Figures

Abbreviations

AFFF Aqueous film forming foams

ECF Electrochemical fluorination

GFF Glass fibre filter

MBBR Moving bed biofilm reactor

PFBA Perfluorobutanoate

PFPeA Perfluoropentanoate

PFHxA Perfluorohexanoate

PFHpA Perfluoroheptanoate

PFOA Perfluorooctanoate

PFNA perfluoronanoate

PFDA Perfluorodecanoate

PFUnDA Perfluoroundecanoate

PFDoDA Perfluorododecanoate

PFTriDA Perfluorotridecanoate

PFTeDA Perfluorotetradecanoate

PFHxDA Perfluorohexadecanoate

PFOcDA Perfluorooctadecanoate

PFBS perfluorobutane sulfonate

PFHxS perfluorohexane sulfonate

PFOS perfluorooctane sulfonate

PFDS perfluorodecane sulfonate

FOSA perfluorooctane sulfonamide

N-MeFOSA N-methyl perfluorooctane sulfonamide

N-EtFOSA N-ethyl perfluorooctane sulfonamide

N-MeFOSE N-methyl perfluorooctane sulfonamidoethanols

N-EtFOSE N-ethyl perfluorooctane sulfonamidoethanols

FOSAA perfluorooctane sulfonamido acetic acid

N-MeFOSAA N-methyl perfluorooctane sulfonamido acetic acid

N-EtFOSAA N-ethyl perfluorooctane sulfonamido acetic acid

FTSA fluorotelomer sulfonate

PFAS Per- and polyfluoroalkyl substances

PFCA Perfluoroalkyl carboxylic acid

PFSA Perfluoroalkyl sulfonic acid

PP Polypropylene

STP Sewage treatment plant

SPE Solid Phase Extraction

WWTP Waste water treatment plant

Acknowledgement

Uppsala Vatten och Avfall AB is thanked for their financial support during the Master project. Eleonora Barck-Holst, Henny Andersson and Conny Karlsson from Uppsala Vatten och Avfall AB are thanked for their help in sampling and data evaluation.

Popular Science Summary

Per-and Polyfluoroalkyl Substances in a Landfill in Uppsala, Sweden.

Per- and polyfluoroalkyl substances (PFASs) are man-made chemicals which are applied as surfactants in many different consumer applications, for instance as repellents in food packaging and textile. Due to their chemical properties, PFASs are extremely persistent, in fact they are not biodegradable in the environment. Landfills are prone to be so called point sources for PFASs to enter the environment since PFAS-containing waste can be deposited on landfills. Subsequently, PFASs can be translocated from the landfill via drainage water into water bodies such as rivers, lakes or even groundwater.

In this particular study it was investigated whether the investigated landfill has an effect on its nearby water systems. PFASs were analysed in drainage water, sewage sludge and groundwater all across the landfill area and in the receiving water courses. Furthermore, an on-site treatment system for the drainage water was assessed in terms of the removal efficiency of PFASs. From our findings we concluded that the landfill had an impact on the nearby aquatic system, in particular the groundwater, but did not show effect on the receiving water system. The treatment system showed efficiencies of around 50% for the simple treatment techniques applied.

Besides their persistency, PFASs were also found to be bioaccumulative and toxic. That means that they accumulate throughout the food chain and in water. For this reason, threshold values for drinking water and groundwater have been introduced for some PFASs by the Swedish National Food Agency and the Swedish Geological Institute respectively. Since the production and application of PFASs is ongoing and PFASs are not degradable under natural conditions their release will steadily pile up and eventually exceed the set thresholds. It is therefore important to study their behaviour in environmental matrices

to develop safe storage or remediation methods and on the other hand to develop efficient treatment methods to guarantee a safe water supply. Thus, operators of waste water treatment plants and waste disposal sites have to deal with the PFASs in their facilities and thereby with the release into the environment. Research on the behaviour of PFASs will contribute to develop and implement efficient treatment systems to avoid the release into the environment and thereby the accumulation of PFASs into the food chain.

1 Introduction

1.1 Per- and polyfluoroalkyl substances

Per- and polyfluoroalkyl substances (PFASs) represent a group of chemicals that have been produced and were used commercially for more than five decades (Jahnke and Berger, 2009). Despite this preceding history, these substances have only received increasing attention on scientific, political and public level in recent years. They have been detected ubiquitously in the natural environment, wildlife and humans all over the world. PFASs are man-made substances featured by their superior stability and therefore by their resistance against all sorts of natural degradation processes. For this reason, several PFASs were found to be bioaccumulative and toxic and to have adverse effects in biota and humans. Due to their unique surface tension lowering potential PFASs were found to be used in a wide range of industrial and commercial products as well as in aqueous film forming foams (AFFFs). Mostly, PFASs are used as surfactants and as surfactant constituents, as which their water, dust and oil repellent properties are perfectly utilized.

1.2 Properties of PFASs

PFASs are organoflourine compounds that are characterized by their high energy carbon-fluorine bond. This bond is an extremely stable polar covalent bond with the negative partial charge on the fluorine atom. In general, these compounds consist of a hydrophobic tail and a hydrophilic head group. Although the carbon-fluorine bond is polar, due to the high electronegativity of the fluorine atom, it is still hydrophobic. The high electronegativity of the fluorine atom makes fluorocarbons very unpolarizable, meaning that fluorine will hold the surrounding electrons very tightly. This also holds true for the carbon-carbon

double bond. Therefore, fluorocarbons interact only weakly with other organic molecules but rather with each other (Rayne and Forest, 2009).

According to Buck et al. (2011), PFASs can be differentiated into polymers and non-polymers. Polymers can be further divides into fluoropolymers, perfluoropolyethers and side-chain fluorinated polymers. Non-polymers are further divided into perfluoroalkyl and polyfluoroalkyl substances. This report only focusses on compounds out of the non-polymer family. These compounds have an alkyl chain of varying length, where the hydrogen atoms are either partially or completely substituted by fluorine atoms. For molecules whose alkyl chain is completely substituted by fluorine atoms we speak of perfluoroalkyl substances, which follow the general formula $F(CF_2)_n - R$, with n as the number of carbon atoms along the alkyl chain and R as the functional head group. Molecules whose alkyl chain is only partially substituted with fluorine atoms are called polyfluoroalkyl substances. In this report, we will focus on these substances that follow the formula $F(CF_2)_n - CH_2CH_2 - R$ (de Voogt and Saez, 2006).

The head group of most perfluoroalkyl substances is either a carboxylic acid (COOH) or a sulfonic acid (SO_3H) group (Rayne and Forest, 2009). In environmental matrices, the acid head groups are usually dissociated which is why these molecules have anionic character (Buck et al., 2011). The ionic PFASs are extremely stable and do not degrade under conditions in the environment (Jahnke and Berger, 2009). However, there are also neutral substances, mostly polyfluoroalkyl substances. In this case either a hydroxide group (OH) or a sulphonamide group is positioned as the head group. In special cases, there can be an ethanol group attached to the sulphonamide group as well (de Voogt and Saez, 2006; van Leeuwen and de Boer, 2007). The non-ionic molecules are also volatile and not persistent to degradation. Due to their volatility, these substances are exposed to long-term transport in the atmosphere and therefor also to deposition in the most remote regions on earth, where they are (a)biotically degraded to their persistent end products. This suggests that a wide range of non-ionic PFASs act as precursor compounds of ionic PFASs (Jahnke and Berger, 2009; van Leeuwen and de Boer, 2007). PFASs exist in a wide range of chain length and branching patterns, depending on their different synthesising method. Alongside the actual compound, a vast number of congeners are produced as well. From an environmental and analytical perspective, these congeners represent a huge challenge for the current research to effectively identify all PFASs present in often very

complicated environmental matrices because decisive synthetic capacities as well as the analytical methods are lacking (Rayne and Forest, 2009).

1.3 Production, usage and regulation of PFASs

PFASs are artificially created chemicals that are used in various types of industrial applications and commercial products. The processes used for the synthesis of PFASs are electrochemical fluorination (ECF) as well as several fluorotelomer oxidation and carboxylation techniques (Prevedouros et al., 2006). By using ECF, both linear and branched isomers were produced, whereas telomerisation yielded linear isomers (Jahnke and Berger, 2009; Paul et al., 2009). The main producers of PFASs are North America, Japan, China, Italy, Germany and Belgium (Paul et al., 2009).

PFASs have been applied in many different industrial and commercial products. For instance, PFASs are used as surfactants on textiles, leather, cookware and paper as their unique aqueous surface tension lowering properties achieve water, oil and dust repellent features. As mentioned above, the ability to create stable foams is used in AFFFs. Furthermore, PFASs are used as metal plating, cleaning, pesticides and many more (Banzhaf et al., 2017; Buck et al., 2011; Prevedouros et al., 2006). According to Paul et al. (2009), the use and disposal of consumer products is responsible for about 85% of indirect release of PFASs into the environment. The remaining 15% are covered by manufacturing release.

The first action to regulate the general release of PFASs has been taken by the main producer, 3M, itself. The company voluntarily decided to terminate the EF production in the year 2000, aiming for a complete phase out by 2002. This especially affected PFOS and related substances. The effectivity of this step is questionable, as the TM-based production has increased since then (de Voogt and Saez, 2006; Paul et al., 2009). Despite the termination of the production, the usage of several products containing PFOS continued. In metal plating, photography and photolithography, semiconductor industries, hydraulic fluids and AFFFs the use was restricted in Europe from December 2007. But even after that some products were still permitted to be used (Paul et al., 2009). In May 2009, PFOS has been added to the persistent organic pollutant list, under annex B of the Stockholm Convention. This resulted in a global restriction of its production and use. The final

phase-out took until 2011 (Banzhaf et al., 2017; Paul et al., 2009).

In Sweden, just within the last few years, an action limit on 11 PFASs in drinking water has been introduced by the National Food Agency. The threshold value has been set to 90 ng/L for perfluorobutane sulfonate (PFBS), perfluorohexane sulfonate (PFHxS), PFOS, 6:2 fluorotelomer sulfonic acid (6:2 FTSA), perfluorobutanoic acid (PFBA), perfluoro-n-pentanoic acid (PFPeA), perfluorohexanoic acid (PFHxA), perfluoroheptanoic acid (PFHpA), PFOA, perfluorononanoic acid (PFNA), and perfluorodecanoic acid (PFDA). Additionally, the Swedish Geological Institute provided a threshold value for groundwater of 45 ng/L and 0.003 mg/kg for sensitive land use (Banzhaf et al., 2017).

1.4 Sources of PFASs

The sources by which PFAS can enter water bodies in environmental systems originate from either point or diffuse sources. Point sources represent locally confined locations, where PFASs are directly introduced into the environment. Such locations can be e.g. waste water treatment plants (WWTPs). These locations are rather well studied and it has been shown that WWTPs are large contributors of PFASs into river systems (Banzhaf et al., 2017). Other point sources are the industrial manufacturing and producing sites, which release PFASs into both aquatic systems and the atmosphere (Prevedouros et al., 2006). Another field of application of PFASs is in AFFFs. Their film forming properties and their resistance to heat make them ideal compounds in fire-fighting applications. Therefore, airports, military bases and fire-fighting training sites can also be classified as point sources with direct release of PFASs into the environment, especially to soil and water (Prevedouros et al., 2006). Landfills are also counted as point sources. As this report is especially investigating landfill leachates, this particular group of point sources is reviewed separately in section 1.5.

Beside the direct release of PFASs via point sources, there can also be an indirect release. In this case it is referred to diffuse sources. These sources, however, are not as clear and more difficult to define. It is suggested that neutral, volatile PFASs such as FTOHs, FOSAs and FOSEs are prone to atmospheric transport and therefore also exposed to both, dry and wet deposition (Ahrens et al., 2011). The deposition can take place pretty much

everywhere, which is why PFASs are deposited in very remote areas as well as urban land. This results in another process following the deposition, surface runoff. In urban regions, this runoff is formed from sealed surfaces whereas in rural areas soil runoff is the dominating process (Ahrens et al., 2011; Banzhaf et al., 2017). The use of PFASs in pesticides contributes to the diffuse release of PFAS in agriculturally cultivated areas.

1.5 Environmental fate of PFASs released from landfills

Landfills have a high potential to be a long-term point source of PFASs entering the environment (Allred et al., 2015; Fuertes et al., 2017). The materials disposed on a landfill, such as municipal solid waste from both domestic and industrial sources, municipal sewage sludge, ashes etc., are prone to contain PFASs. After their disposal, they are exposed to chemical reactions, degradation processes and precipitation, possibly throughout a period of a few decades. The percolation process allows the water to take up PFASs and dislocate them into the leachate (Busch et al., 2010; Fuertes et al., 2017; Yan et al., 2015). The translocation process, however is influenced by several factors such as pH, electrical conductivity and precipitation (Benskin et al., 2012). Nowadays, landfills are usually equipped with or connected to wastewater treatment plants (WWTPs), where the leachate is handled. However, the question about the efficiency of these treatment processes remains open, simply since most effective treatment methods, such as adsorption on activated black carbon, are not implemented into the treatment process in most of the cases which pose a risk for the environment (Allred et al., 2015; Yan et al., 2015). Some studies have shown that WWTPs even increase the concentration of PFCAs and PFSAs in the effluent compared to the influent due to the biodegradation of precursor compounds (Ahrens et al., 2011; Busch et al., 2010). The degradation of precursors in general is proposed as an important factor contributing to the presence of stable end products, such as PFCAs and PFSAs, in landfill leachates (Benskin et al., 2012; van Zelm et al., 2008). Another pathway on which PFASs can enter the environment is atmospheric release from both WWTPs and landfills (Ahrens et al., 2011). According to this study the compounds most prone to atmospheric release are the neutral fluorotelomer alcohols. Among landfills, however, there can be great differences in PFASs concentrations of the leachate. Huset et al. (2011) suggests that the range of concentration is strongly dependent on the kind of waste they receive, for example higher PFAS concentrations in leachates are expected

if the waste is linked to fluorochemical manufacturing processes (Huset et al., 2011). The composition profiles of landfill leachates also show considerable variabilities but most studies have shown that PFCAs are the major constituent in landfill leachates. For example, Li et al. (2012) identified short chain PFCAs as the major substances present, accounting for 73% of the total amount of PFASs.

1.6 Goal of this study

The goal of the present study was to assess the occurence and distribution profiles of PFASs on a typical swedish landfill. The investigation on PFASs on the landfill site was studied for leachate, groundwater and sludge. Special attention was payed on the on-site sewage treatment system and its efficiency for the removal of PFASs. Furthermore the mass flow of PFASs along the receiving water course was estimated. A suggestion of the influence of the landfill to nearby as well as the further distant environment based on these investigations will be given.

2 Material and methods

2.1 Analysed PFASs

In total, 28 PFASs were analysed (Table 1). For the quantification, an internal standard mix (FXIS11) (Table 2) was used.

2.2 Sampling

2.2.1 Description of the sampling site - Hovgården Landfill

Hovgården Landfill is located approximately 12 km northeast of Uppsala and covers an area of 570000 m^2 (Figure 2.1). The landfill exists since 1971, and was built to dispose ashes from a nearby incineration plant located in Uppsala. In the southwestern part of the area, the "old landfill" is situated (referred to "old landfill" in this thesis). The old landfill (127000 m^2) is not active anymore, meaning that no further material is filled in there and it is in the process of being sealed. In the old landfill mainly ashes, construction waste and contaminated soil were deposed. In the north close to the old landfill the compost process and storage is located (38000 m^2). In this part, compost and organic waste is treated in three different steps (i.e hygenisation, composting and separating.). The most western part of the area is used for wooden waste. In the centre of the landfill is currently used for waste disposal (this part is referred to "active landfill" in the following) (61000 m^2). At this site, mainly insulation material and plaster are deposed. Ashes are stored on the landfill area before they are separated from metal. The gravel which is left is used for the construction of the old landfill. In between the western boarder of the active landfill and the compost platform, space for non-permanent storage of combustion waste is located.

Table 2.1: Analysed per- and polyfluoroalkyl substances

Name	Abbreviation	Molecular formula
PFCAs (perfluoroalkyl carboxylated)		
perfluorobutanoate	PFBA	$C_3F_7CO_2^-$
perfluoropentanoate	PFPeA	$C_4F_9CO_2^-$
perfluorohexanoate	PFHxA	$C_5F_{11}CO_2^-$
perfluoroheptanoate	PFHpA	$C_6F_{13}CO_2^-$
perfluorooctanoate	PFOA	$C_7F_{15}CO_2^-$
perfluorononanoate	PFNA	$C_8F_{17}CO_2^-$
perfluorodecanoate	PFDA	$C_9F_{19}CO_2^-$
perfluoroundecanoate	PFUnDA	$C_{10}F_{21}CO_2^-$
perfluorododecanoate	PFDoDA	$C_{11}F_{23}CO_2^-$
perfluorotridecanoate	PFTriDA	$C_{12}F_{25}CO_2^-$
perfluorotetradecanoate	PFTeDA	$C_{13}F_{27}CO_2^-$
perfluorohexadecanoate	PFHxDA	$C_{15}F_{31}CO_2^-$
perfluorooctadecanoate	PFOcDA	$C_{17}F_{35}CO_2^-$
PFSAs (perfluoroalkane sulfonates)		
perfluorobutane sulfonate	PFBS	$C_4F_9SO_3^-$
perfluorohexane sulfonate	PFHxS	$C_6F_{13}SO_3^-$
perfluorooctane sulfonate	PFOS	$C_8F_{17}SO_3^-$
perfluorodecane sulfonate	PFDS	$C_{10}F_{21}SO_3^-$
FOSAs (perfluorooctane sulfonamides)		
perfluorooctane sulfonamide	FOSA	$C_8F_{17}SO_2NH_2$
N-methyl perfluorooctane sulfonamide	N-MeFOSA	$C_8F_{17}SO_2N(CH_3)H$
N-ethyl perfluorooctane sulfonamide	N-EtFOSA	$C_8F_{17}SO_2(C_2H_5)H$
FOSEs (perfluorooctane sulfonamidoethanols)		
N-methyl perfluorooctane sulfonamidoethanol	N-MeFOSE	$C_8F_{17}SO_2(CH_3OH)H$
N-ethyl perfluorooctane sulfonamido-ethanol	N-EtFOSE	$C_8F_{17}SO_2(C_2H_5OH)H$
FOSAAs (perfluorooctane sulfonamidoacetic acids)		
perfluorooctane sulfonamido acetic acid	FOSAA	$C_8F_{17}SO_2NH_3CH_2CO_2H$
N-methyl perfluorooctane sulfonamido acetic acid	N-MeFOSAA	$C_8F_{17}SO_2NCH_3CH_2CO_2H$
N-ethyl perfluorooctane sulfonamido acetic acid	N-EtFOSAA	$C_8F_{17}SO_2N(CH_2)_3CH_3CO_2H$
FTSAs (x:2 fluorotelomer sulfonates)		
6:2 fluorotelomer sulfonate	6:2 FTSA	$C_8H_4F_{13}SO_3^-$
8:2 fluorotelomer sulfonate	8:2 FTSA	$C_{10}H_4F_{17}SO_3^-$
10:2 fluorotelomer sulfonate	10:2 FTSA	$C_{12}H_4F_{21}SO_3^-$

Table 2.2: Internal Standards and injection standard

Internal Standard	Corresponding PFASs
$^{18}O_2$ PFHxS	6:2 FTSA, PFHxS
$^{13}C_4$ PFOS	PFBS, PFDS, PFOS
$^{13}C_4$ PFBA	PFBA
$^{13}C_2$ PFHxA	PFPeA, PFHxA
$^{13}C_4$ PFOA	PFHpA, PFOA
$^{13}C_5$ PFNA	PFNA
$^{13}C_2$ PFDA	PFDA
$^{13}C_2$ PFUnDA	PFUnDA
$^{13}C_2$ PFDoDA	PFDoDA, PFTriDA, PFTeDA, PFHxDA, PFOcDA
$^{13}C_8$-FOSA	FOSA
d_3-N-MeFOSA	N-MeFOSA
d_5-N-EtFOSA	N-EtFOSA
d_3-N-MeFOSAA	FOSAA, N-MeFOSAA
d_5-N-EtFOSAA	N-EtFOSAA
d_7-N-MeFOSE	N-MeFOSE
d_9-N-EtFOSE	N -EtFOSE
Injection Standard	
$^{13}C_8$PFOA	

This waste will be transported to combustion plants when required. In the southern part, close to the entrance gate of the area, there is a sorting platform for industrial waste as well as a sorting plant (19000 m^2). The sorting plant is not in use anymore, the sorting is done by excavators. Furthermore, there is a small domestic recycling plot and one for chemical waste. In the northern part of the landfill, the "soil cell" (19500 m^2) and the "sludge cell" (19500 m^2) are located. In these cells, contaminated soils and dried sewage sludge from WWTPs in Uppsala are stored. East of the sludge there is the area called Svartmuttern. In this area, wet sludge from WWTPs as well as sludge directly removed from the municipal sewage system is brought there to drain (1700 m^2). The WWTP as well as several ponds included in the sewage treatment process are situated in the eastern part. Besides, there are also some storage platforms for stones and gravel for building purposes, metal, drainage pipes, diesel tanks etc.

The waste water treatment system at Hovgården landfill combines several separated treatment steps including aeration, Moving Bed Biofilm Reactor (MBBR), sedimentation pond, polishing ponds/lakes and oxidation pond.

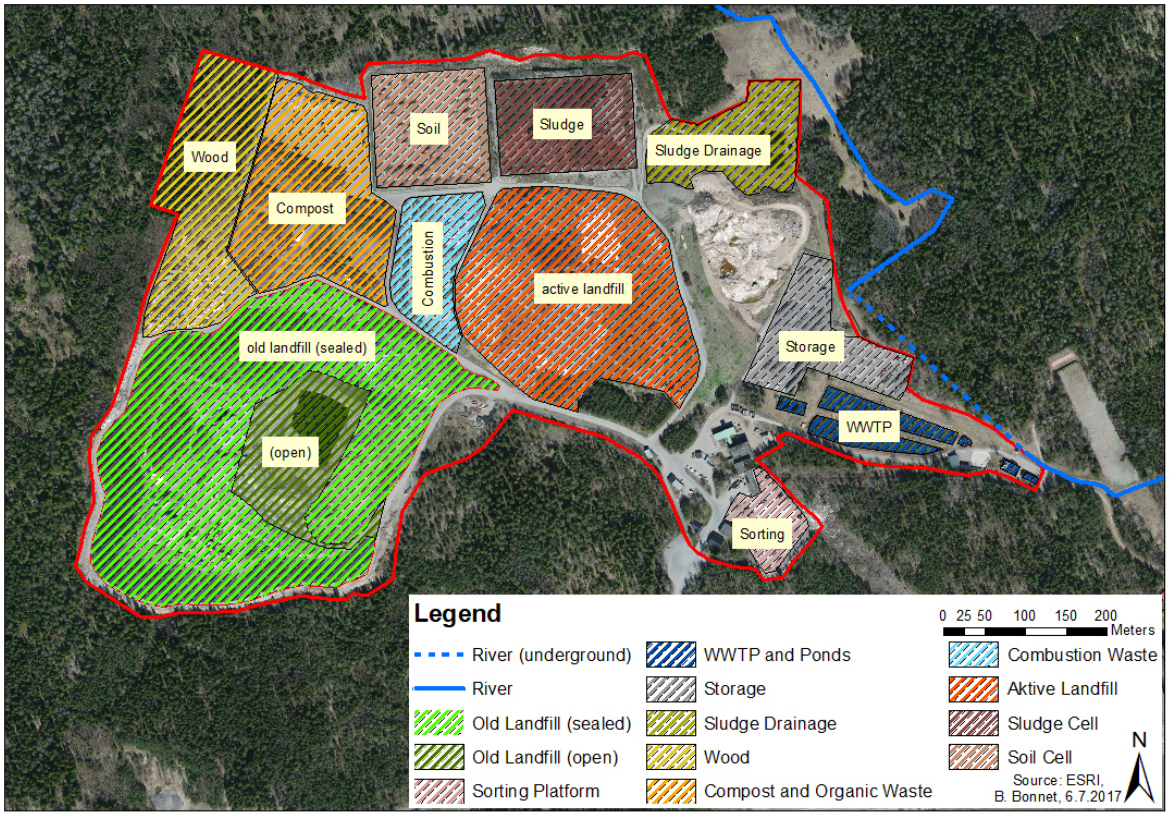

Figure 2.1: Hovgården Landfill

Aeration. The combined sewage from the drainage system enters the WWTP. Then, the sewage runs through an aeration step. This step is rather short (10-15 min) and its function is the oxidation of iron and manganese. The oxidation processes results in the formation of flocs, which will be seperated from the sewage after the oxidation step, when the sewage is running over a lamella system. The sludge is then brought to Svartmuttern to drain.

Moving Bed Biofilm Reactor (MBBR). After the aeration, the sewage is treated in a MBBR. In this treatment step many special plastic carriers are introduced into an aeration tank. The plastic carriers represent a surface where a biofilm can grow on. The density of the carriers is somewhat close to water and due to the aeration, these carriers have good floating abilities and are therefore in good contact with the sewage. In this case, the microbial community is represented by autotrophic bacteria, also called nitrifiers. These bacteria convert ammonium to nitrite (NO_2) and then nitrate (NO_3) through various biological

processes using dissolved oxygen. The nitrification step is usually followed by a denitrification step; however, this step is not implemented in the treatment system at Hovgården.

Sedimentation Pond, Polishing Lakes and Oxidation Pond. After the treatment in the MBBR, the sewage is pumped to a sedimentation pond, where any remaining flocs and solids are given time to settle down with a retention time of about 20 hours. After the sedimentation pond, the sewage is pumped into two polishing lakes, each with a retention time of about 20 days. They act as some kind of "wetland", where bacteria and plants use some organic and inorganic compounds for their growth. As a last treatment step, the sewage is brought into an oxidation pond. In this step, the oxygen level of the sewage is elevated in order to not cause reductive conditions in the receiving water course.

After this last treatment, the water exits the landfill and flows into the environment.

2.2.2 Sampling design and sampling information

All samples were taken in February and March 2017. Besides the time integrated sampling, all other liquid samples with grab water sampling methods. The sampling containers were 1 L PP bottles. Prior to sampling 1 L PP bottles were rinsed with methanol 3 times in the laboratory. In the field, 1 L PP bottles were rinsed 3 times with the sample liquid before taking the final sample. The samples were stored in insulated boxes during transportation. Until analysis in the laboratory, the samples were stored in the refriderating room at SLU. No replicates have been made.
Samples from the drainage system were taken with the sampling bottles attached to a rope with a weight in the lower end. Thereby a penetration below a water surface was ensured. Groundwater samples were taken with a diving pump, pneumatic circulation pump attached to a battery drill and bailors.

2.2.2.1 Sampling at the landfill and drainage system

In Figure 2.2 the sampling locations for the landfill and the STP are presented. The goal for the sampling on the site was to get representative grab water samples from the drainage system. Ideally, this meant to get separate samples from each section on the site. To follow

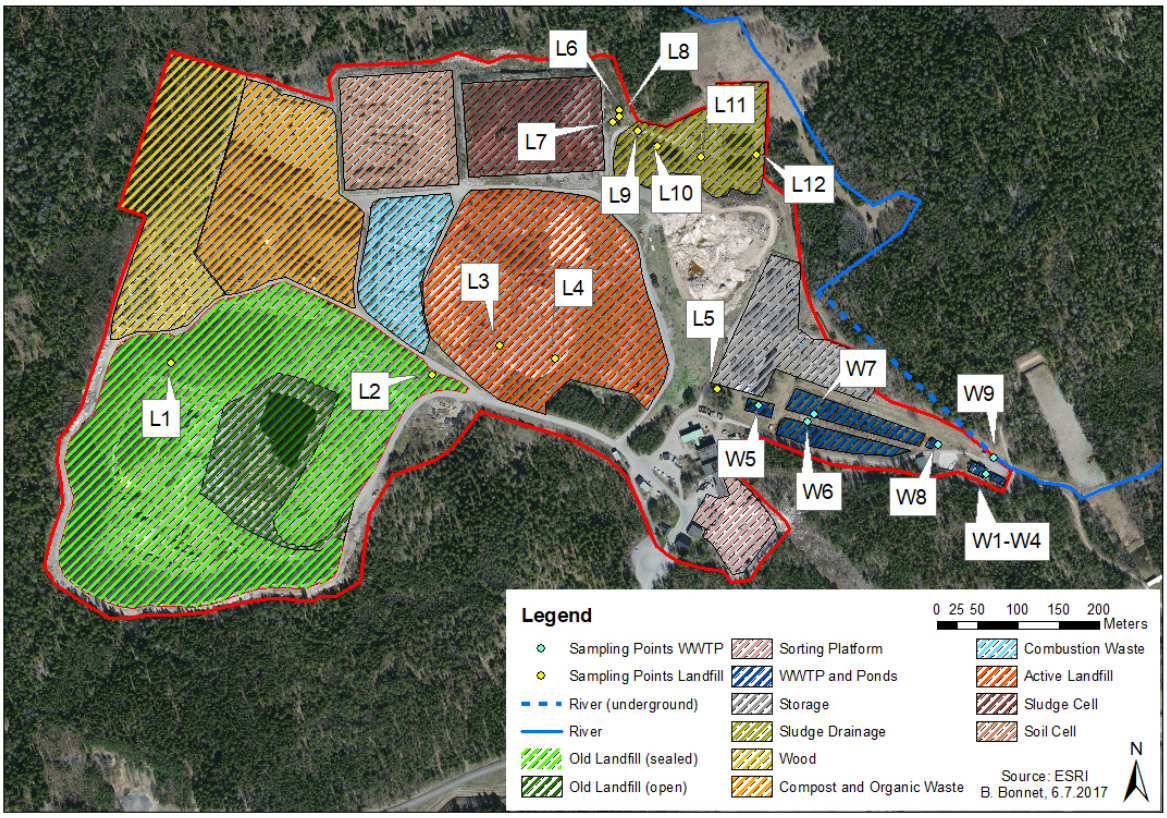

Figure 2.2: Sampling locations: landfill and STP

up which of the sections is mentioned, a schematic plan of the landfill is presented in Figure 2.3.

The drainage of the Hovgården is basically divided into two sections. The areas which are separately drained are presented as A and B (Figure 2.3). Area A includes the sections old landfill, wood, compost and active landfill. Unfortunately, the different sections were not individually accessible by wells. The only well that was easily accessible for sampling was L5, where the drainage system for the entire area A could be sampled. Samples from area A also included one sample from the drainage system of the old landfill, L1, as well as one sample from the drainage of the surface that has been covered partially already, L2. On the active landfill, two more samples, L3 and L4, were taken from the drainage system. The drainage system on both landfills were accessed via tubes reaching down to the bottom of the system.

Area B includes the soil and the sludge cells as well as the area 'sludge drainage'. In this part, easier accessible sampling sites allowed a more precise sampling. The sewage of both the soil cell and the sludge cell were sampled separately at L6 and L7 respectively. From sampling point L8, which is located in a little house, and onwards the sewage of the soil and the sludge cells was combined. Sample L9 was taken from a well constructed out of a wide plastic tube before the sewage enters a sedimentation pond. Sample L10 was taken after the first sedimentation pond, again from a wide plastic well. After L10, the sewage enters another sedimentation pond. Sample L11 was sampled after the second sedimentation pond. The sewage for the entire red area was then sampled at the location L12. L5 and L12 represent the last sampling locations where the sewage from area A and area B, respectively is collected. Thereafter, the sewage is combined and flows towards the WWTP. The sewage from the sorting platform for industrial waste is separated and enters the drainage system after L5. However, there was no sample taken from this area.

The influent to the WWTP was sampled at location W1. A sample were collected after the aeration (W2). Then, the sewage is separated into two MBBRs, and samples were collected after each reactor, at location W3 and W4. Further on, the sewage is pumped to a sedimentation pond (W5), followed by two sedimentation lakes (W6 and W7) were sampled. After the lakes, the sewage enters the last treatment step, the oxidation pond, where another sample was taken at W8. Then the water leaves the landfill at sampling site W9. Shortly after the exit, another sample was taken at location R3 (see chapter 2.2.4 River sampling).

Time integrated sampling was used for the locations L5 and L12 as well as for W1 and W9. The time integrated sampling was performed using the machines ISCO 6712 Portable Sampler (Teledyne ISCO, Lincoln, USA). They were programmed to take a 300ml sample each hour over the duration of one day, to form one composite sample. For the locations D0 and S0 the sampling was conducted from April 3rd 12:00 until April 4th 12:00 and for the locations R1 and A1 from April 4th 13:30 until April 6th 13:30

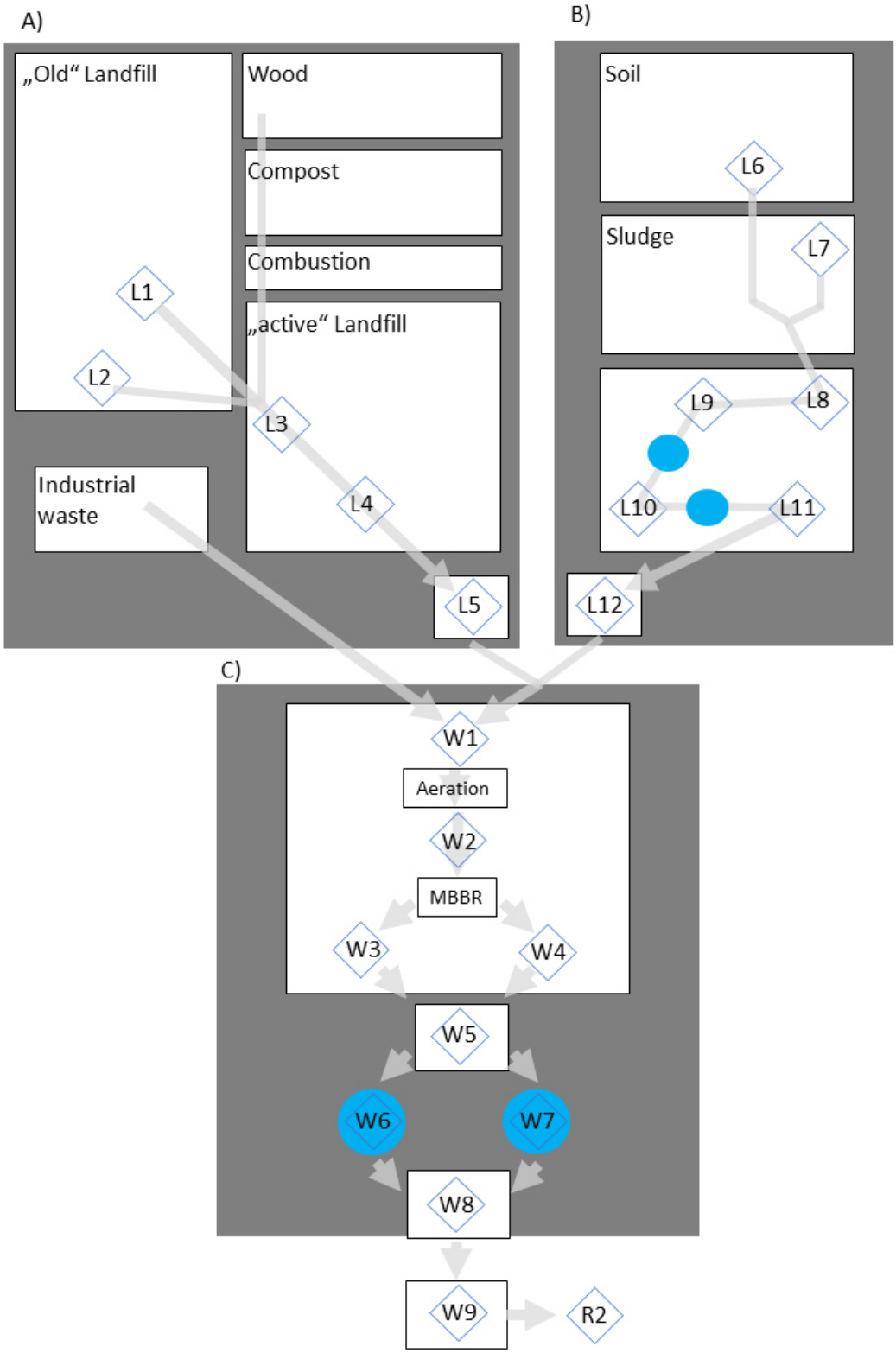

Figure 2.3: Schematic sampling plan

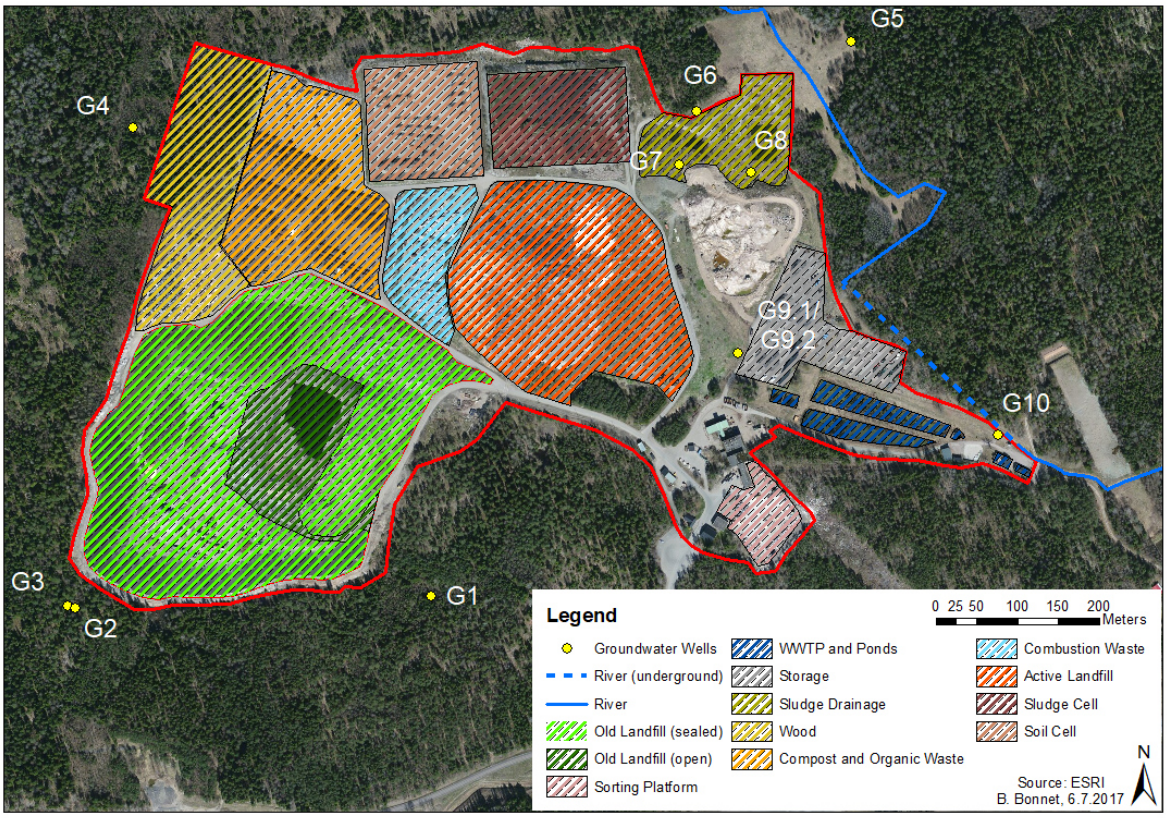

Figure 2.4: Groundwater sampling locations

2.2.2.2 Groundwater sampling

Several groundwater samples have been taken at Hovgården landfill including on the landfill site (G6-G10) and outside of the landfill site (G1-G5) (Figure 2.4). The main direction of the groundwater flow is from west to east. The groundwater sites G1-G5 were considered as less impacted since they were located upstream of the main groundwater flow (east to west).

G1 (3.1 m depth) is located southeast of the old landfill, the part where construction and industrial waste was deposited. G2 (4.8 m) is located at the southwestern side of the old landfill, where ashes have been disposed. G3 (0.5 m) was an additional well sampled at the southwestern corner of the old landfill, right beside G2. G4 (0.5 m) is located in the woods approximately 50 m west of the platform for wooden waste. G5 (1 m) is also located outside of the landfill area, approximately 100 m northeast of the area Svartmuttern. The

wells G6 (2.05 m), G7 (1.6 m) and G8 (2.8 m) are situated east of the sludge cell in the area Svartmuttern. G6 is located north of the two sedimentation ponds for the sewage from the soil and the sludge cells. G7 is located north of the sedimentation ponds. G8 is located south of the drainage basins for the sludge from the municipal sewage system. Sampling site G9 is located east of the active landfill. At this sampling location two different wells are situated. G9.1 (8.1 m) is referred to as the outer well, whereas G9.2 (8 m) is referred to as the inner well. G9.1 and 9.2 are vertically seperated by an impermeable barrier, preventing water to leak from the active landfill. The barrier is supposed to push the leaking water into the direction of L5, where the water then enters the drainage system. G9.2 is the well inside (west) of the barrier and G9.1 outside of the barrier (east). The last groundwater well G10 (4.05 m) is located at the eastern part of the landfill, close to the WWTP and the exit of the sewage at W9.

2.2.2.3 River sampling

In order to follow up the fate of the drainage water of the landfill in the environment, the receiving water course has been sampled. Nine samples have been taken all along the way to lake Ekoln (Figure 2.5). After the sewage exited the landfill at W9, a sample was taken at R2 which was just 100 m down the stream from W9. The next sampling location, R3, was located close to Fribacken. 8 kilometres downstream close to Landbro, sampling site R4 was located. At Funbo, 6 kilometres further downstream, sampling site R5 was situated. The next sampling location was R6 close to Grönviken, 3.5 kilometres further downstream. Nearby Edebybro, sampling location R7 was situated, with a distance to W9 of 18 kilometres. The following sample, R9, was taken at the river Fyrisån, at a location before the river Sävjaån entered the Fyrisån. Close by, at the outlet of the river Sävjaån, sample R8 was taken. 30 kilometres downstream, in Flottsund sample R10 was taken. The last sample R11 was taken after the outlet of the Fyrisån river in lake Ekoln.

Two samples have been taken before the drainage water of the landfill entered the stream. North of the landfill the small stream Hovgårdsbäcken emanates. This stream, however, is only running on the surface for a short while until it is led underground. The point at which it was led underground is located at R1. The stream then runs underground until after the exit of the drainage water of the landfill and shortly before W9, the underground stream was sampled at R1.

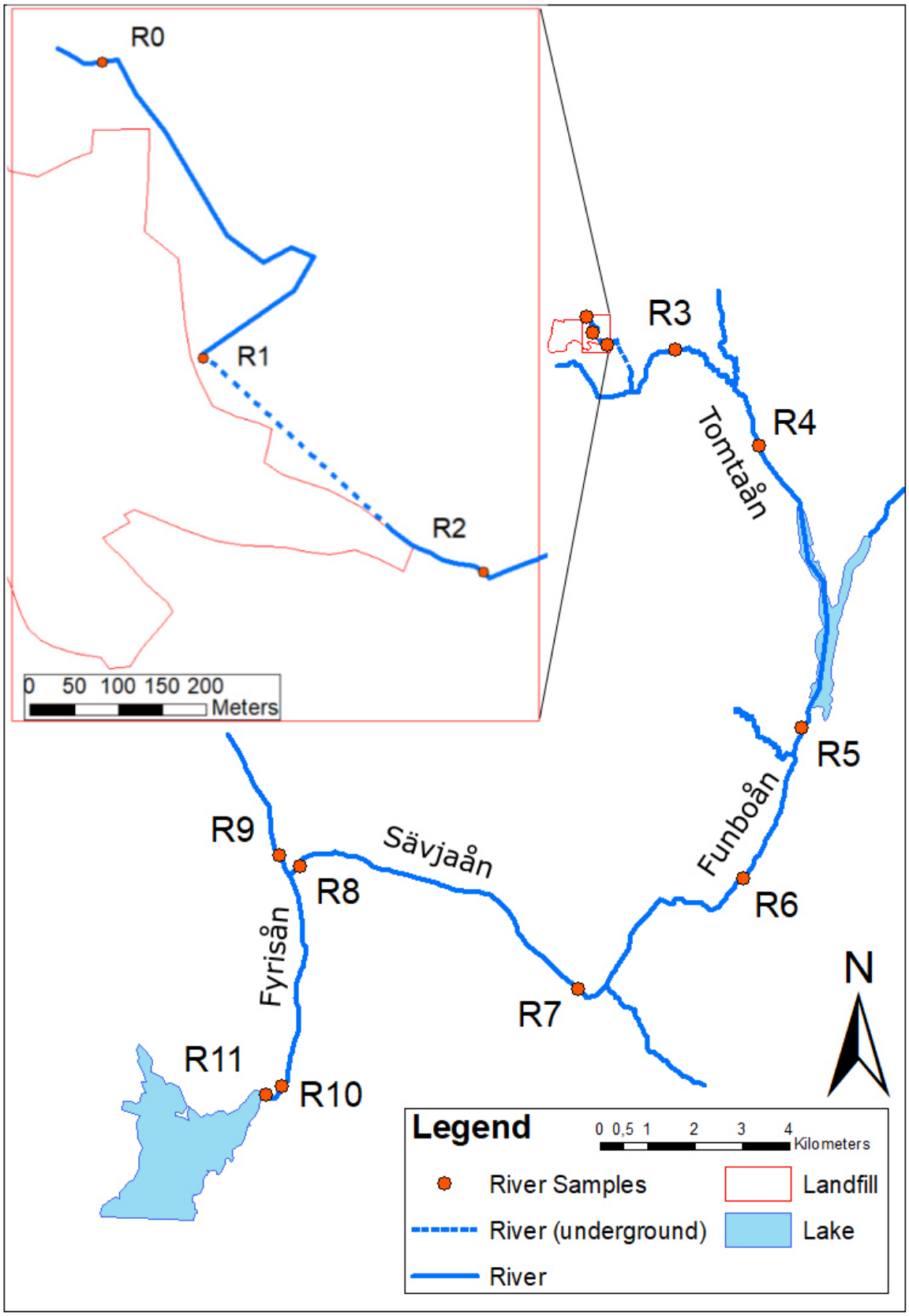

Figure 2.5: River sampling locations

2.2.2.4 River flow data

The flow data for the investigated rivers was obtained as modelled data from "SMHI vattenweb", Sweden (www.http://vattenwebb.smhi.se/). This model estimates the flow data for catchments. Modelled flow data existed for the points F4-F10 (Figure 6.1). These points represent outlet points of local catchments, for which the outflow was modelled on a daily basis. The coordinates of the sampling points did not match the coordinates of the assigned points of the model. Therefore, the closest modelled outflow point was taken as a reference for each sampling point. The outflow of the uppermost catchment was modelled at F4. In order to achieve a more detailed estimation of the flow rates further upstream, the flow rate F4 and F0 were estimated as fraction of the total outflow of the catchment, modelled for F5, according to the runoff area corresponding to the sampling points. Therefore, the runoff area only contributing to the sampling points were estimated. Proportionally to the whole area, the flow rate for each individual sampling point could be estimated. The flow rates are presented in table 6.1. It has to be mentioned that the modelled data have uncertainties with an error between 25% and 36% according to SMHI vattenweb. The area based estimation of the smaller catchments was conducted by reference to a topographic map in ArcMap. This was a rather rough estimation and might therefore also deficient.

2.3 Sample preparation

2.3.1 Water samples

2.3.1.1 Filtration

The glassware filtration equipment was washed in the dishwasher and baked out in the oven at 400°C. The glass fibre filters (GFFs) from $Whatman^{TM}$ (particle size = 1.2 µm) were burned in the oven at 400°C. Before use, the filtration equipment was rinsed three times with gradient grade methanol from Merck (Darmstadt, Germany, 99.9 %).The GFFs were placed with the "wavey" side facing up. Before filtration, the samples were sonicated for five minutes. When the GFFs were blocked, they were replaced by a new filter. For samples with a lot of particles, ten 50 mL PP tubes were filled with the sample and centrifuged at

2500 rpm for 3 minutes. The supernatant was then filtrated. The filtration was conducted under vacuum with a speed of 5 mL min^{-1}. 500 mL (±10%) were filtrated and filled into 1 L PP bottles, which have been rinsed three times with methanol and weighed prior to filtration. The filtration funnel was then rinsed three times with methanol. The methanol was then transferred into the same 1 L PP bottle. The same was done for the glass bottle of the filtration equipment. In between the filtration of different samples, the used filtration equipment was rinsed six times with methanol.

2.3.1.2 Solid phase extraction

Prior to the extraction, cartridge adapters and stop cocks were rinsed in methanol twice by sonication for 15 min. SPE manifold, syringes (reservoirs), adapters and stop cocks were rinsed with methanol three times and dried by air directly before start. Two solutions have been prepared. Ammonium acetate buffer was prepared from 170 mL 25 mM acetic acid, which was prepared from 0.25 mL acetic acid (100%) purchased from Merck (Darmstadt, Germany) and 174.75 mL Millipore Water, and 30 mL 25mM ammonium acetate, prepared from 0.058 g ammonium acetate (99%) obtained from Sigma-Aldrich (Sweden) and 30 mL Millipore water. Millipore Water was acquired through a Milli-Q Advantage Ultrapure Water purification system (Millippore, Billercia, MA). The second solution, 0.1% ammonium hydroxide in methanol, was prepared from 99.6 mL methanol and 0.4 mL 25% ammonium hydroxide in solution from Sigma-Aldrich (Sweden).

The Solid Phase extraction (SPE) was performed for all water samples using an Oasis WAX cartridge (6 cc, 500 mg 60 µm, Waters). The cartridge was preconditioned with 4 mL of 0.1 % ammonium hydroxide in methanol and 4 mL of methanol to clean and condition the cartridge. Then, 4 mL Millipore water was added onto the cartridge to adjust for the solvent conditions of the samples. In the following step, approximately 500 mL of filtrated water sample, which was spiked with 100 µL mass-labelled internal standard (c = 20 pg $µl^{-1}$) before, was loaded onto the cartridge. The flow rate was adjusted to approx. 1 drop per second using vacuum. After the loading ran through the cartridge a washing step with 4 mL of 25 mM ammonium acetate buffer in methanol was done to remove salts from the cartridge that could interfere in the following steps of the analysis. The cartridges were then dried for 2 min at 3000 rpm in the centrifuge. The last step of the SPE was the elution step. The extract was eluted into 15 mL PP tubes that were cleaned 3 times with methanol

prior the SPE. First, the cartridge was loaded with 4 mL of methanol and secondly with 8 mL 0.1 % ammonium hydroxide in methanol. The elution was very carefully conducted only using the vacuum when it was necessary. When the elution was done, the vacuum was turned on to dry out the cartridge. The sample extract in the 15 mL PP tubes were concentrated under nitrogen stream. The samples were evaporated to below 1 mL within the PP tubes. Tubes were then rinsed twice with methanol and again concentrated to below 1 mL. The remaining volume was then transferred to a 2 mL brown glass vial (Agilent Technologies). The PP tubes were then rinsed three times with methanol and the volume was added to the glass vial. In the glass vial the samples were then concentrated to 0.5 mL.

For each SPE batch a laboratory blank was prepared (in total n = 5). For the blank, the cartridge was preconditioned, washed, and dried as described above (but not loaded with a water sample). Then, the 100 µL of the mass-labelled internal standard (c = 20 pg μl^{-1}) was spiked before the elution step as described above.

2.3.2 Solid samples

The sludge samples were filled into 50 ml PP tubes and were then freeze-dried for one week. All PP tubes were rinsed three times with methanol prior use. After freeze-drying, the samples were homogenized and 3 g were weighed into another 50 mL PP tube. In the following step 2 mL of 100 mM sodium hydroxide in 80%/20% methanol/Millipore water was added and soaked for 30 minutes. 100 mM sodium hydroxide was prepared by diluting 0.5 g sodium hydroxide (97%) purchased in pellets from Sigma-Aldrich (Sweden) in 50 mL Millipore water. After that 20ml methanol and 100 µL of mass-labelled internal standard (c = 20 pg μl^{-1}) were added. The closed tube was then sonicated for 30 min followed by centrifugation at 3000 rpm for 15 min. The supernatant was then decanted into another 50 mL PP tube. The extraction was then repeated by adding 1 mL of 100 mM sodium hydroxide in 80%/20% methanol/Millipore water and soaking for 30 min. After that 10ml methanol were added into the PP tube. Again, the samples were sonicated for 30 min and centrifuged at 3000 rpm for 15min. The supernatant was added into the second PP tube. The tube was shaken by hand after 0.1 mL 4M hydrochloric acid was added into the tube. The 4M hydrochloric acid was prepared by mixing 4.09 mL of concentrated hydrochloric acid (30%) from Merck (Darmstadt, Germany) with 10 mL Millipore water. 8.3 mL of the extract were transferred from the second 50 ml PP tube into a 15 mL PP tube before

concentrating the sample under nitrogen stream to 0.5 mL. A 1.7 mL Eppendorf centrifuge tube was prepared with 25 mg ENVI-carb (120/400, Supraclean ENVIcarb SupELCO) and 50µl glacial acetic acid (100%) from Merck (Darmstadt, Germany). The 0.5 mL extract from the 15 mL was transferred into the Eppendorf centrifuge tube and vortex-mixed for 30 sec. Then the Eppendorf tube was centrifuged at 4000 rpm for 15 min before the supernatant was transferred into an autoinjector vial.

2.4 Instrumental analysis for PFASs

PFASs were analysed using Ultra Performance Liquid Chromatography (UPLC) coupled with a tandem mass spectrometer (MS/MS). Electrospray Ionisation was used in negative mode. The instrument on which the analysis was performed was TSQ Quantiva by Thermo Scientific (Thermo Scientific, Waltham, MA, USA). A reverse-phase Waters Acquity UPLC BEH C18 (2.1 x 50 mm, 1.7 µm particle size, Waters) column was used as the stationary phase. The flow rate of the mobile phase was held constant at 0.5 $\mathrm{mL\,min^{-1}}$. The mobile phase consisted solvent A (Millipore water with 5 mM ammonium acetate) and solvent B (acetonitrile). Gradient elution was used with 98% solvent A and 2% solvent B as initial conditions. Initial conditions were held for 0.5 min. After that the composition of the mobile phase was change towards solvent B. After 8 min constant increase the composition was 2% solvent A and 98% solvent B. These conditions were kept for 2 min. After that, initial conditions were set and kept for 2 min. This results in a total time of analysis of 12 min. The injection volume was 10 µl. Column temperature was set to 40°C.

3 Results

3.1 Qualitiy control and quality assurance

Table 3.1: Internal standard recoveries with standard deviations (%) in water and sludge

Internal Standard	water (n=5) (%)	sludge (n=5) (%)	Corresponding PFASs
$^{18}O_2$ PFHxS	70 ± 16	47 ± 6	6:2 FTSA, PFHxS
$^{13}C_4$ PFOS	81 ± 15	49 ± 16	PFBS, PFDS, PFOS
$^{13}C_4$ PFBA	7 ± 6	35 ± 7	PFBA
$^{13}C_2$ PFHxA	34 ± 14	45 ± 5	PFPeA, PFHxA
$^{13}C_4$ PFOA	58 ± 17	45 ± 3	PFHpA, PFOA
$^{13}C_5$ PFNA	70 ± 13	37 ± 4	PFNA
$^{13}C_2$ PFDA	70 ± 12	30 ± 8	PFDA
$^{13}C_2$ PFUnDA	57 ± 14	27 ± 5	PFUnDA
$^{13}C_2$ PFDoDA	38 ± 14	25 ± 4	PFDoDA, PFTriDA, PFTeDA, PFHxDA, PFOcDA
$^{13}C_8$-FOSA	63 ± 14	24 ± 5	FOSA
d_3-N-MeFOSA	17 ± 10	31 ± 7	N-MeFOSA
d_5-N-EtFOSA	15 ± 10	29 ± 7	N-EtFOSA
d_7-N-MeFOSE	33 ± 11	40 ± 13	N-MeFOSE
d_9-N-EtFOSE	28 ± 11	31 ± 12	N -EtFOSE
d_3-N-MeFOSAA	77 ± 21	42 ± 7	FOSAA, N-MeFOSAA
d_5-N-EtFOSAA	75 ± 23	38 ± 7	N-EtFOSAA
Average recovery (%)	50 ± 14	36 ± 7	

To ensure the quality and correctness of the analysis, standard recoveries (Table 3.1) as well as average blank concentrations, method detection limits (MDL) (Table 3.2) were calculated. The recovery for both water (50%) and sludge (36%) were rather low. Landfill leachate is often accompanied by large matrix effects. These effects will have influence

Table 3.2: Average PFAS concentrations with standard deviations and method detection limits for the blank samples

	Water ($ng\,L^{-1}$)		Sludge ($ng\,g_{dw}^{-1}$)	
Analyte	avg. blank conc. (n=48)	MDL	avg. blank conc. (n=9)	MDL
PFBA	0.51 ± 0.13	1.81	0.51 ± 0.11	0.29
PFPeA	0.58 ± 0.32	3.11	0.58 ± 0.29	0.48
PFHxA	0.40 ± 0.22	2.12	0.40 ± 0.19	0.33
PFHpA	0.04 ± 0.021	0.21	0.04 ± 0.018	0.03
PFOA	1.1 ± 0.016	2.35	1.1 ± 0.014	0.39
PFNA	nd	0.02	nd	0.0033
PFDA	nd	0.02	nd	0.0033
PFUnDA	0.016 ± 0.022	0.17	0.016 ± 0.019	0.03
PFDoDA	nd	0.02	nd	0.0033
PFTriDA	nd	0.02	nd	0.0033
PFTeDA	nd	0.02	nd	0.0033
PFHxDA	0.17 ± 0.14	1.20	0.17 ± 0.13	0.18
PFOcDA	0.20 ± 0.21	1.69	0.20 ± 0.19	0.26
PFBS	0.06 ± 0.06	0.52	0.06 ± 0.06	0.08
L-PFHxS	0.03 ± 0.009	0.10	0.03 ± 0.0079	0.02
B-PFHxS	nd	0.02	nd	0.0033
L-PFOS	nd	0.02	nd	0.0033
B-PFOS	nd	0.02	nd	0.0033
PFDS	nd	0.02	nd	0.0033
10:2 FTSA	0.50 ± 0.26	2.5	0.50 ± 0.23	0.39
8:2 FTSA	nd	0.02	nd	0.0033
6:2 FTSA	0.70 ± 0.016	1.50	0.70 ± 0.014	0.25
L-FOSA	0.019 ± 0.02	0.16	0.019 ± 0.018	0.02
B-FOSA	nd	0.02	nd	0.0033
Me-FOSA	nd	0.02	nd	0.0033
Et-FOSA	nd	0.02	nd	0.0033
Me-FOSE	0.02 ± 0.03	0.24	0.02 ± 0.03	0.04
Et-FOSE	0.40 ± 0.5	3.7	0.40 ± 0.5	0.57
FOSAA	0.37 ± 0.0048	0.77	0.37 ± 0.0043	0.13
Me-FOSAA	0.013 ± 0.012	0.09	0.013 ± 0.01	0.01
Et-FOSAA	nd	0.02	nd	0.0033

during sample preperation and instrumental analysis. This could be one reason for these low recoveries.

The blank concentrations in water ranged between nd (not detected) and 1.1 $ng\,L^{-1}$ (PFOA) and the MDL between 0.02 and 3.7 $ng\,L^{-1}$ (Et-FOSE). In the sludge samples

the blank concentrations ranged between nd and 0.37 ng g_{dw}^{-1} (Et-FOSE) with MDL of 0.0033 and 0.57 ng g_{dw}^{-1}.

3.2 PFASs in landfill leachate

The landfill samples were analysed for 28 PFASs. For the landfill section A and B, 23 PFASs were identified (Figure 3.1). The substances PFHxDA, PFOcDA, PFDS, 10:2 FTSA, Me-FOSA, Et-FOSA, Me-FOSE and Et-FOSE were not detected. The highest PFAS concentration was measured for the time integrated sample at L5, with 1600 ng L^{-1}. The overall detection frequency for short-chain $C_3 - C_6$ PFCAs as well as PFOA, PFNA and PFDA were >90% in area A. In area B, PFBA was only detected in L12. Long-chain $C_7 - C_{17}$ PFCAs were only detected at L1 in concentrations below 1 ng L^{-1}. PFOA (in average 120 ng L^{-1}, median: 46 ng L^{-1}) and PFHxA (120 ng L^{-1}, 100 ng L^{-1}) showed the highest average concentrations, followed by PFBA (57 ng L^{-1}, 3.7 ng L^{-1}). PFSAs were frequently detected in both areas with higher average concentrations in area A. PFDS was not present in any sample. PFOS was the most abundant compound for both isomers with the linear PFOS (in average 50 ng L^{-1}, median: 23 ng L^{-1}) and the branched PFOS (45 ng L^{-1}, 11 ng L^{-1}), followed by the short-chain compound PFBS (52 ng L^{-1}, 19 ng L^{-1}). PFHxS was the least abundant compound (in average 34 ng L^{-1}, median: ng L^{-1} linear and 8.0 ng L^{-1}, 2.1 ng L^{-1} branched). Among the precursor compounds, 6:2 FTSA was the most abundant substance (in average: 130 ng L^{-1}, median: 60 ng L^{-1}). The highest concentration was identified at L7 (630 ng L^{-1}). The abundancy for 6:2 FTSA was higher in area B with an average concentration of 190 ng L^{-1} (median: 140 ng L^{-1}), compared to area A with an average of 41 ng L^{-1} (53 ng L^{-1}).

The composition profile shows the relative contribution of each substance to the total concentration. The most abundant class of PFASs for the entire area A were the PFCAs. The contribution of the PFCAs ranges from 45% (of the $\sum$PFASs) for L2 up to 69% for the time integrated sample at L5. The most contributing single substance in area A was PFOA (in average 23% for L1-L5), followed by PFHxA (17%), PFBA (11%), PFHpA (6%), PFPeA (5%) and the remaining PFCAs were below 1%. PFSAs account for an average of 28% (of the $\sum$PFASs) in the samples in area A, with PFBS as the most contributing single substance (10%), followed by the linear (7.0%) and the branched (6.3%) isomer of

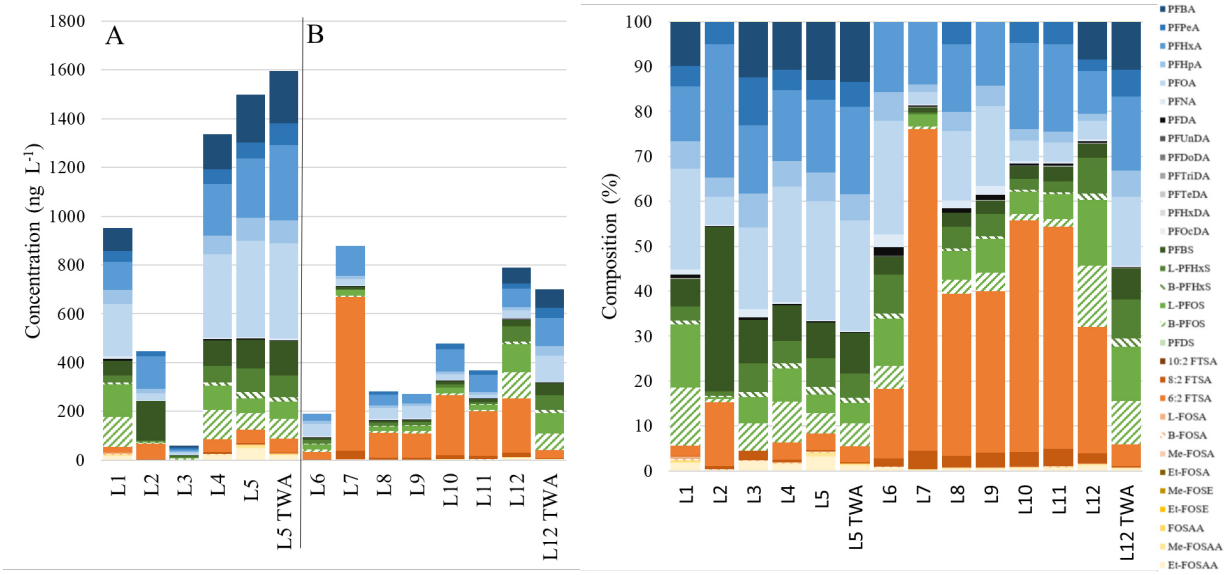

Figure 3.1: Total concentration and composition profile of the leachate

PFOS. In area B, the most abundant class of substances were FTSAs, averaging 42% of the ∑PFASs. At four of the seven sampling locations L7 (76%), L9 (39%), L10 (55%) and L11 (53%) FTSAs were identified as the main contributors. PFCAs were the largest contributor at the locations L6, L8 and the time integrated sample at L12, with 43%, 52% and 55%, respectively. PFSAs accounted for the largest part in the grab water sample at L12 (41%). PFSAs also accounted for more than 39% in the time integrated sample at L12. The most abundant single substance in all samples was 6:2 FTSA (in average 39% for L7-L12). At L6 PFOA (25%) and in the time integrated sample at L12 PFHxA (17%) were the most contributing substances.

In area A, the sampling locations on the active landfill, L4 and L3 showed high differences of their ∑PFAS concentration levels with 1335 ng L^{-1} and 59 ng L^{-1}, respectively. The sample L1, from the bottom of the drainage system of the old landfill, accounted for ∑PFAS 951 ng L^{-1} and L2, representing the outflow of parts of the surface drainage, contained ∑PFASs of 447 ng L^{-1}. The separated drainage system of area B, which involved the soil and the sludge cells, showed a maximum concentration at L7 with ∑PFASs of 879 ng L-1. The soil cell sewage L6 had ∑PFAS concentrations of 190 ng L^{-1}. After the confluence of the sewage of both the soil and the sludge cells, ∑PFAS concentrations of 282 ng L^{-1} at L8 and 272 ng L^{-1} at L9 were measured. ∑PFAS concentrations were 480 ng L^{-1} and 370 ng L^{-1} after the first (L10) and the second (L11) sedimentation pond,

respectively. The second and third highest ∑PFAS concentrations were measured at L12 with a slightly higher concentration in the grab water sample (790 ng L^{-1}) compared to the time integrated sample (701 ng L^{-1}).

3.3 PFASs in sludge

In the sludge samples, 23 out of 31 PFASs have been identified (Figure 3.2). The substances that were not detected were PFBA, PFPeA, branched PFHxS, PFDS, Me-FOSA, Et-FOSA, Me-FOSE and Et-FOSE. Total ∑PFAS concentrations ranged from 33 ng g_{dw}^{-1} (February 2017) to 440 ng g_{dw}^{-1} (August 2016). In the sludge from April and May 2016 ∑PFAS concentrations ranged between 100 ng g_{dw}^{-1} to 82 ng g_{dw}^{-1}. In August 2016, an increased ∑PFAS concentration to 440 ng g_{dw}^{-1} was found and in the sludge from September and October 2016 a concentration of 190 ng g_{dw}^{-1} and 230 ng g_{dw}^{-1}, respectively, was measured. The concentrations from November 2016 to February 2017 were in the range of 75 ng g_{dw}^{-1}.

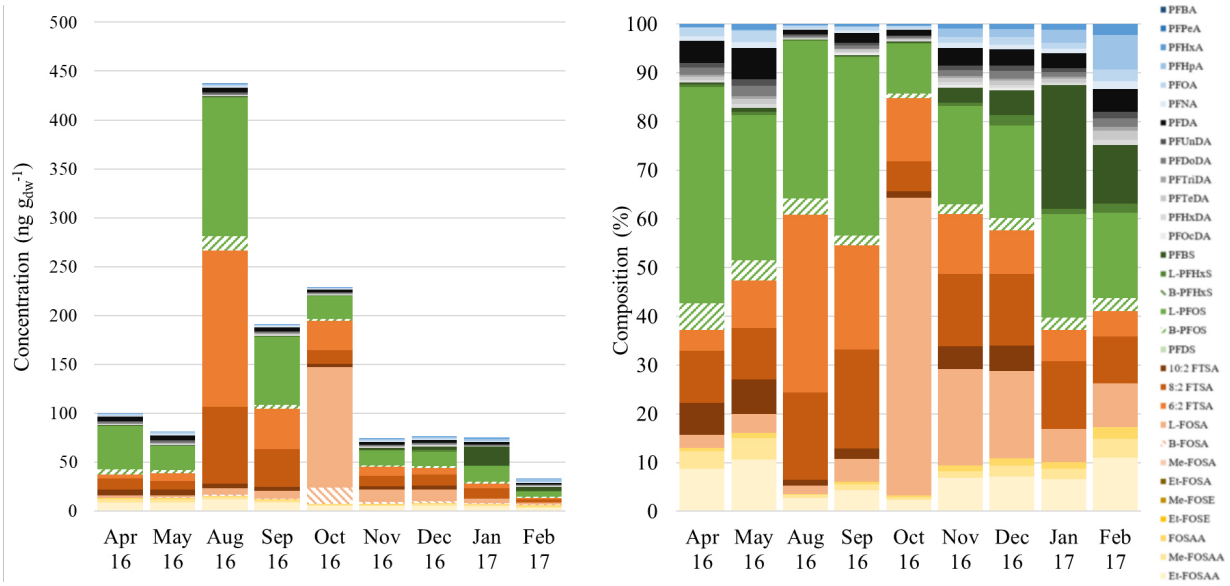

Figure 3.2: Total concentration and composition profile of the sludge

The dominating group in the sludge samples were FTSAs with an average contribution of 37% of the ∑PFASs, followed by PFSAs (33%), FOSAs (15%) and PFCAs (7.6%). The highest average concentration for a single substance was identified for the linear isomer of

PFOS (in average: 40 ng g_{dw}^{-1}, median: 24 ng g_{dw}^{-1}) accounting for 28% of the $\sum$PFASs. In the group of FTSAs, 6:2 FTSA, second most abundant single substance, (in average: 30 ng g_{dw}^{-1}, median: 7.9 ng g_{dw}^{-1}) and 8:2 FTSA (20.8 ng g_{dw}^{-1}, 11 ng g_{dw}^{-1}), both contributing in average with 20% and 14% of the $\sum$PFASs, respectively. 10:2 FTSAs (in average 3.5 ng g_{dw}^{-1}, median: 4.04 ng g_{dw}^{-1}) was only present in the sludge samples. Linear and branched FOSA were measured with in average 19 ng g_{dw}^{-1} (median: 6.5 ng g_{dw}^{-1}) and 2.8 ng g_{dw}^{-1} (median: 1.03 ng g_{dw}^{-1}), accounting for 13% and 2.01% of the $\sum$PFASs respectively. FOSAAs were measured with in average concentration of 10 ng g_{dw}^{-1} (6.9% of the $\sum$PFASs) including Et-FOSAA (in average: 6.9 ng g_{dw}^{-1}, median: 5.5 ng g_{dw}^{-1}), Me-FOSAA (2.1 ng g_{dw}^{-1}, 1.8 ng g_{dw}^{-1}), FOSAA (0.9 ng g_{dw}^{-1}, 0.8 ng g_{dw}^{-1}). $\sum$PFCAs showed only an average of 11 ng g_{dw}^{-1} (in average, 7.6% of $\sum$PFASs). The contribution of short-chain C_3–C_7 PFCAs was lower (in average, 1.7% of the $\sum$PFASs) compared to the water samples L1-L12 (in average, 4.4% of the $\sum$PFASs). PFBA and PFPeA were not detected in any sludge samples. Therefore, in the solid samples the long-chain C_8–C_{17} PFCAs had a rather high contribution (in average, 6.5% of the $\sum$PFASs). The only compound that was not detected in every sludge sample was PFOcDA. PFDA was the most abundant compound with in average 3.3 ng g_{dw}^{-1} (in average, 30% of the $\sum$PFCAs) followed by PFOA 1.4 ng g_{dw}^{-1} (12%) and PFDoDA 1 ng g_{dw}^{-1} (10%).

3.4 PFASs in the STP and removal efficiency

In the sewage of the WWTP, 19 out of 31 investigated PFASs could have been identified. PFUnDA, PFDoDa, PFTriDa, PFTeDa, PFHxDa, PFDS, 10:2 FTSA, Me-FOSA, Et-FOSA, Me-FOSE, Et-FOSE and FOSAA have not been detected in any sample (Figure 3.3). Total $\sum$PFAS concentrations ranged from 66 ng L^{-1} (W4) to 1100 ng L^{-1}(W1 TWA). The highest $\sum$PFAS concentration was in the influent to the STP at W1 for both, the time integrated (1100 ng L^{-1}) and the grab sample (1008 ng L^{-1}). In the following treatment step, the aeration (activated sludge), the concentration dropped to 760 ng L^{-1} at W2. The samples after the treatment (MMBR) W3 (640 ng L^{-1}) and W4 (66 ng L^{-1}) showed a considerable difference. In the sedimentation pond W5 and the sedimentation lakes, W6 and W7, $\sum$PFAS concentration of 630 ng L^{-1}, 301 ng L^{-1} and 436 ng L^{-1}, respectively, were detected. In the last treatment step, the oxidation pond at W8, $\sum$PFAS

concentration increased to 669 ng L^{-1}. The sewage exits the site at W9 where ∑PFAS concentrations of 630 ng L^{-1} in the time integrated sample and 530 ng L^{-1} in the grab water sample were identified. Further in the stream at R2, ∑PFAS concentration further drops to 437 ng L^{-1}.

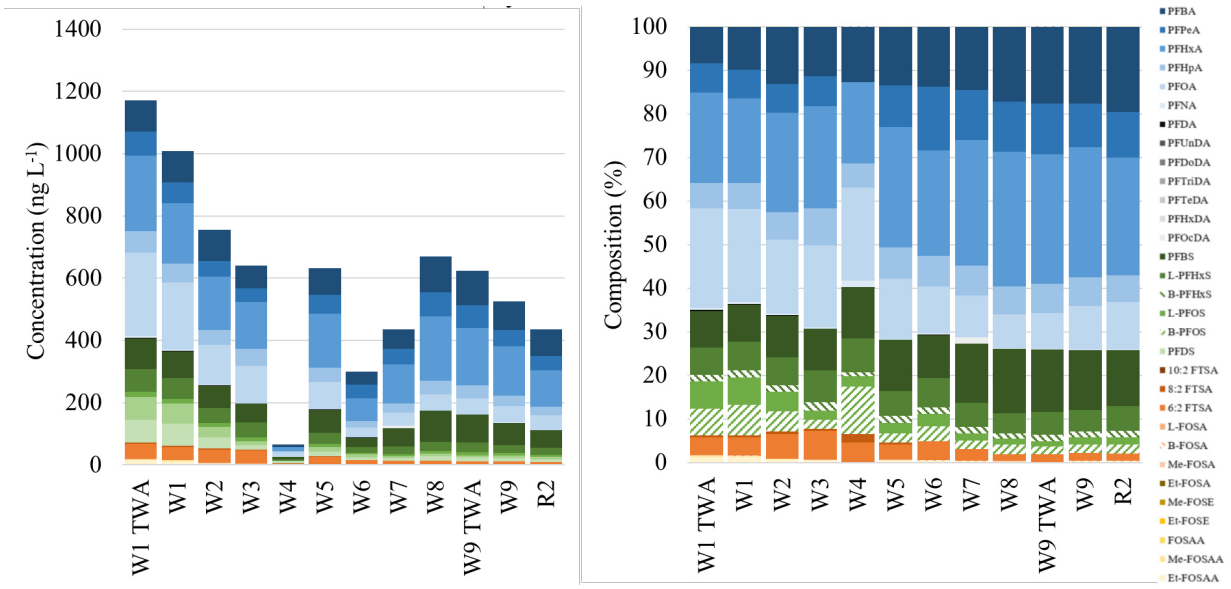

Figure 3.3: Total concentration and composition profile in the STP

The most abundant class of PFASs were PFCAs with a sum concentration of in average 420 ng L^{-1} (69% of the ∑PFASs). PFSAs (in average 150 ng L^{-1}) made up 26% and precursors (averaging 29 ng L^{-1}) 5% of the ∑PFAS concentration. Among the PFCAs, PFHxA was the most abundant compound with 150 ng L^{-1} (25% of the ∑PFASs), followed by PFOA 93 ng L^{-1} (15%), PFBA 81 ng L^{-1} (13%), PFPeA 53 ng L^{-1} (8.8%) and PFHpA 40 ng L^{-1} (6.5%). PFNA and PFDA combined accounted for less than 1%. Except the absent PFDS, all PFSAs were detected in every sample. The short-chain PFBS was the most abundant (in average 67 ng L^{-1}) accounting for 43% of ∑PFSAs. Total PFHxS and total PFOS concentration made up for 29% and 28% of ∑PFSAs respectively, with average concentrations of 36 ng L^{-1} and 21 ng L^{-1} for the linear isomer and 9.2 ng L^{-1} and 23 ng L^{-1} for the branched, respectively. Within the group of precursor compounds, 6:2 FTSA was the most abundant compound with in average 22 ng L^{-1} (3.6% of ∑PFASs), followed by Et-FOSAA with 3.8 ng L^{-1} (0.62% of ∑PFASs).

The removal efficiency showed a total removal efficiency for ∑PFASs of 47% (W1 TWA

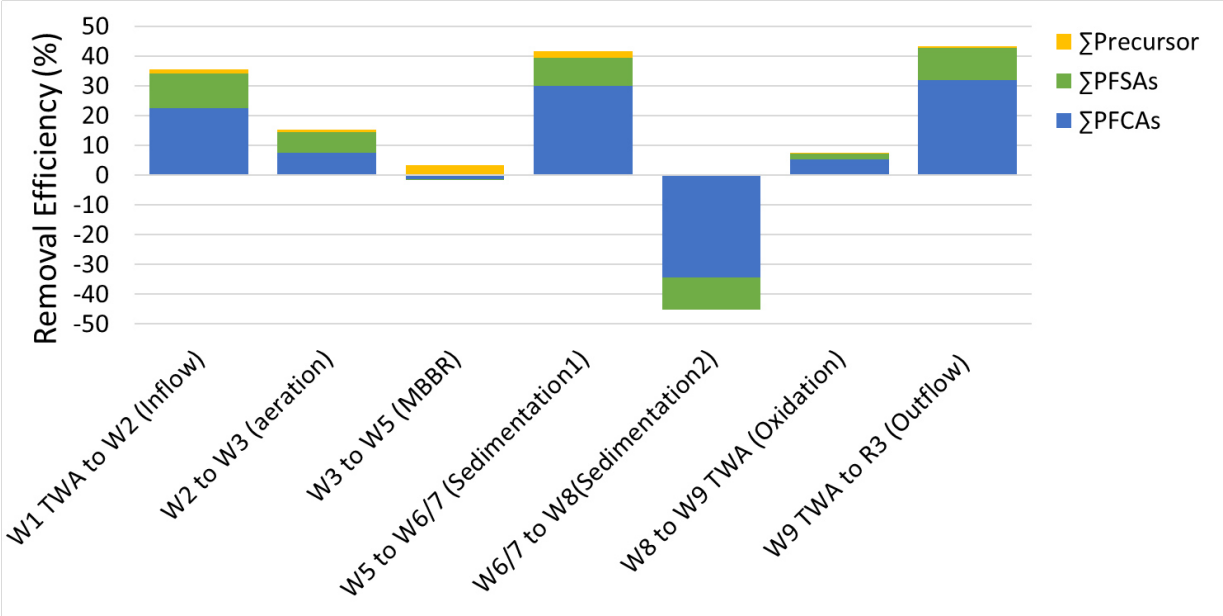

Figure 3.4: Removal efficiency between the treatment steps

to W9 TWA). The removal efficiency for PFCAs, PFSAs and precursor compounds were 40%, 55% and 84%, respectively. ∑Precursor concentration constantly decreased after each treatment step. The highest removal efficiency rates for precursors were identified after the sedimentation pond (42%) and after the aeration treatment (36%)(Figure 3.4). PFCAs were most efficiently removed in the sedimentation pond as well (30%) whereas 9.4% removal efficiency for PFSAs accounted for the second most efficient treatment step of PFSAs. PFSAs were most efficiently removed in the aeration step with 12%. In the polishing ponds however, the ∑PFASs concentration increased by 45% (indicated by the negative removal efficiency). After exiting the landfill between W9 and R3 43% of the ∑PFASs were removed.

PFDA, 8:2 FTSA, Me-FOSAA and Et-FOSAA all show removal efficiencies of 100% (Figure 3.5). PFOA, PFNA, PFOS and 6:2 FTSA all show removal efficiencies between 70-90%. Long-chain PFCAs and PFSAs are more efficiently removed that their short-chain counterparts. For PFCAs, the removal efficiency of PFBA (C_3 PFCA) was negative with -10% and constantly increased with up to 100% for PFDA (C9 PFCA). For PFSAs, the removal efficiency of PFBS (C_4) was 9.6% and increased with up to 90% for the linear isomer of PFOS. For the PFAS precursors the removal efficiency was generally high ranging from 53% for the linear isomer of FOSA over the branched isomer of FOSA (66%) and 6:2FTSA

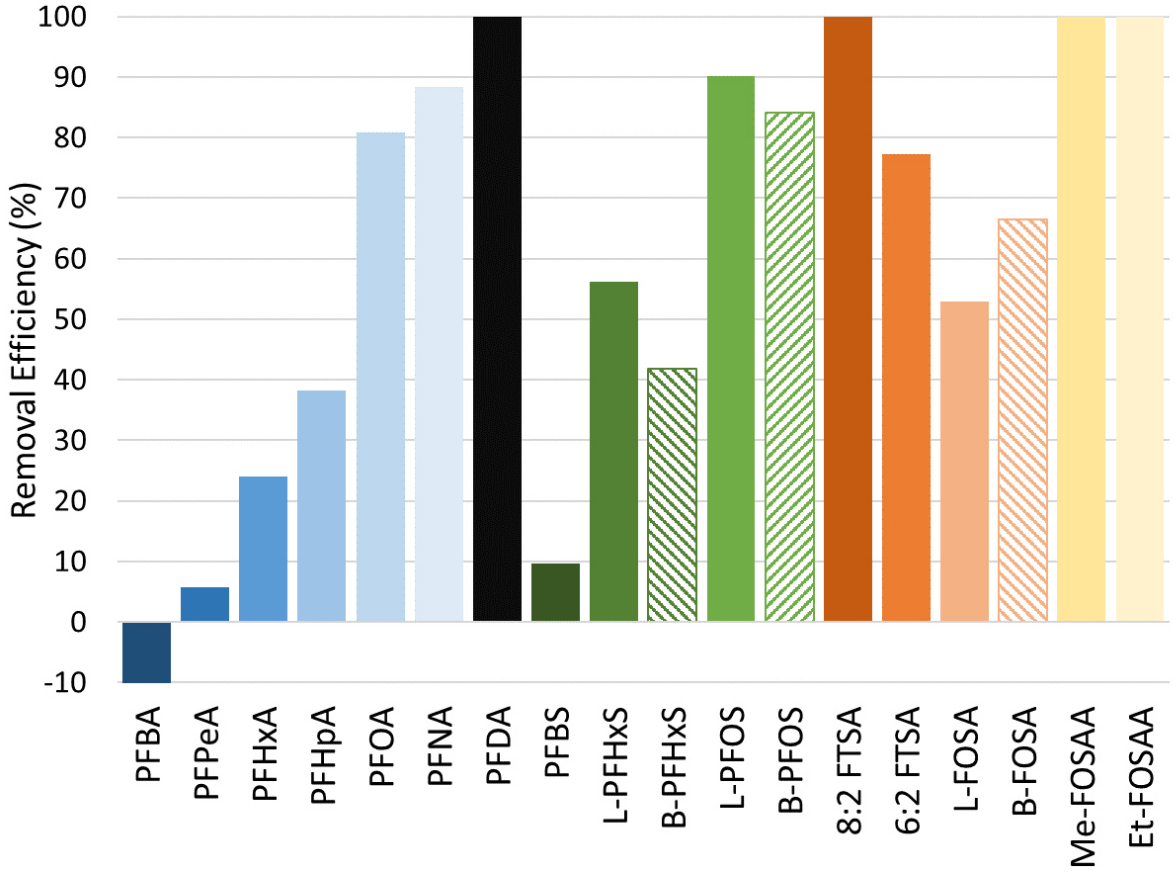

Figure 3.5: Removal efficiency for PFASs between W1 (influent STP) and W9 (effluent STP)

(77%) up to 100% for 8:2 FTSA, Me-FOSAA and Et-FOSAA.

3.5 PFASs in the groundwater

In the groundwater samples, 19 of 31 analysed PFASs were present. PFUnDA, PFDoDA, PFTeDA, PFHxDA, PFDS, 10:2 FTSA, Me-FOSA, Et-FOSA, Me-FOSE, Et-FOSE and FOSAA were not detected (Figure 3.6). PFTriDA was only present in sample G1. $\sum$PFASs concentrations ranged from 8.5 ng L^{-1} (G5) up to 1800 ng L^{-1} (G9.2). The highest $\sum$PFAS concentration was identified at G9.2 (1800 ng L^{-1}), followed by G9.1 (540 ng L^{-1}), G6 (460 ng L^{-1}), G2 (340 ng L^{-1}), G3 (309 ng L^{-1}), G8 (300 ng L^{-1}), G10 (150 ng L^{-1}), G7 (96 ng L^{-1}), G1 (85 ng L^{-1}), G4 (42 ng L^{-1}) and G5 (8.5 ng L^{-1}). The concentration at G9.2

was the highest concentration detected in any sample taken on the landfill site.

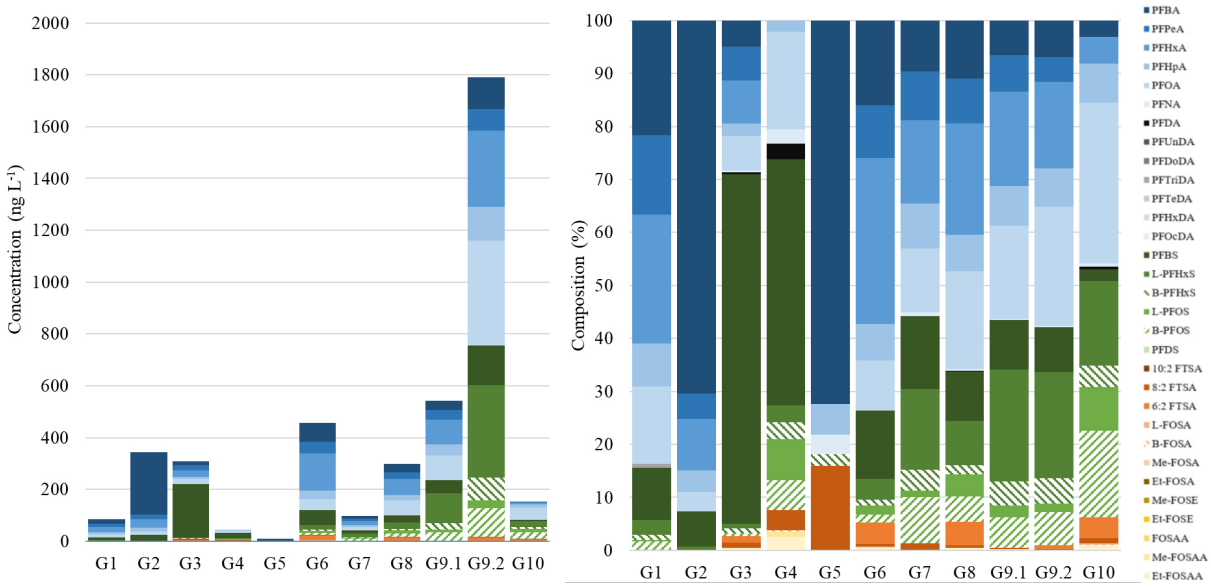

Figure 3.6: Total concentration and composition profile for the groundwater

The most abundant class of PFASs were PFCAs with an average concentration of 230 ng L^{-1} (61% of $\sum$PFASs). PFSAs with an average concentration of 140 ng L^{-1} and precursors with 7.5 ng L^{-1} accounted for 37% and 2%, respectively, of $\sum$PFASs. PFOA and PFHxA showed the highest average concentrations both measured with 64 ng L^{-1} (17% of $\sum$PFASs), followed by PFBA with 51 ng L^{-1} (14%), PFHpA with 25 ng L^{-1} (6.6%) and PFPeA with 23 ng L^{-1} (6.04%). PFHxS was the most abundant PFSA with average concentrations of 51 ng L^{-1} (14% of $\sum$PFASs) and 12 ng L^{-1} (3.3% of $\sum$PFASs) for the linear and the branched isomer, respectively. Both isomers combined for 17% of $\sum$PFASs and 45% of $\sum$PFSAs. PFBS had an average concentration of 51 ng L^{-1} (14% of $\sum$PFASs) and PFOS 26 ng L^{-1} for both linear and branched isomers (7% of $\sum$PFASs). Precursor concentrations were generally low with an average concentration of 7.5 ng L^{-1} (2% of $\sum$PFASs). The most abundant precursor was 6:2 FTSA with an average concentration of 5 ng L^{-1} (1.3% of $\sum$PFASs).

3.6 PFASs in river

In the river samples, 19 out of 31 analysed PFASs were identified (Figure 3.7). PFUnDA, PFDoDA, PFTeDA, PFHxDA, PFOcDA, PFDS, 10:2 FTSA, Me-FOSA, Et-FOSA, Me-FOSE, Et-FOSE and FOSAA were not present. The sample R2 is not present in this section as this sample was taken shortly after the outlet of the landfill, the concentration was too high (440 ng L^{-1}), to be properly visualized in Figure 3.7. Therefore, it was included into the part of the STP. However, the sample R3 should be referred to as the sampling location with the highest concentration in the river. Total ∑PFASs concentrations ranged from 0.3 ng L^{-1} (R6) to 41 ng L^{-1} (R1). The highest concentration was identified at R1, the sampling location before the effluent from the landfill entered the receiving water course. Sampling locations R3 and R4 had ∑PFASs concentrations of 29 ng L^{-1} and 4.2 ng L^{-1}, respectively. The samples R5-R7 were measured with total ∑PFASs below 1 ng L^{-1}. In the following samples R8-R11 ∑PFASs concentrations of 3.3 ng L^{-1}, 7.9 ng L^{-1}, 6.2 ng L^{-1} and 6.02 ng L^{-1} respectively were detected.

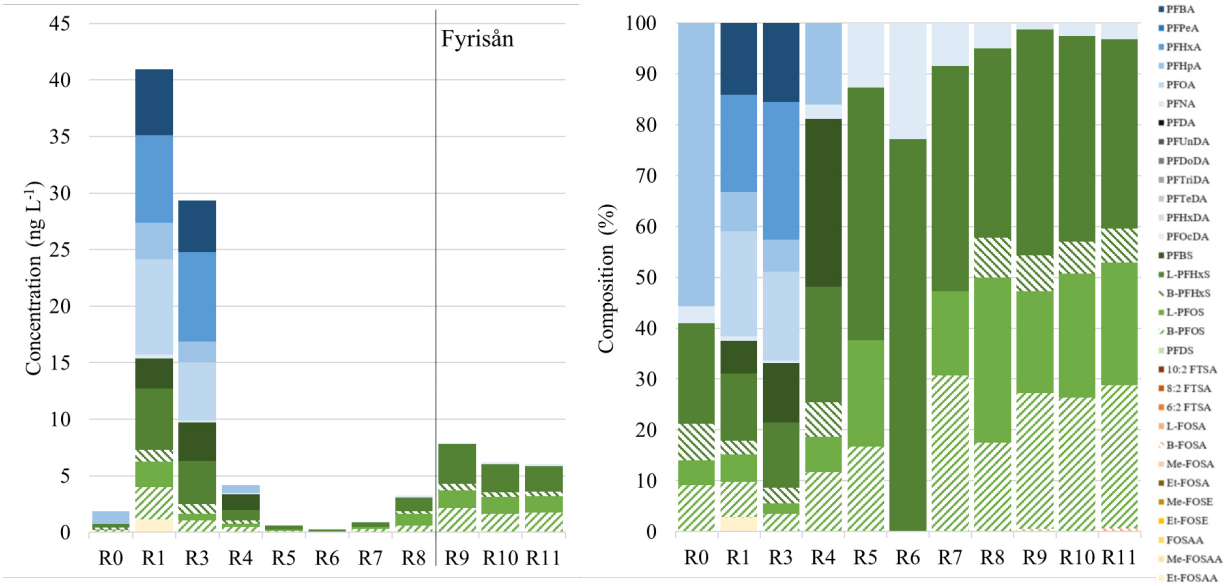

Figure 3.7: Total concentration and composition profile for the river

The most abundant class of PFASs were PFSAs (in average 4.8 ng L^{-1}, 52% of ∑PFASs). Average concentrations of PFCAs and precursors were 4.4 ng L^{-1} (47% of ∑PFASs) and 0.11 ng L^{-1} (1% ∑PFASs) respectively. PFHxA (in average 1.4 ng L^{-1}, 15% ∑PFASs)

and PFOA (1.2 ng L^{-1}, 13% of the ∑PFASs) were the most abundant compounds among PFCAs. PFSAs were more frequently detected with PFHxS as the most abundant compound with 1.9 ng L^{-1} for the linear PFHxS (21% of the ∑PFASs) and 0.36 ng L^{-1} for the branched PFHxS (3.9%), followed by PFOS with 0.83 ng L^{-1} (8.4% ∑PFASs) and 0.99 ng L^{-1} (10.8% ∑PFASs) for the linear and the branched isomer, respectively. ∑Precursos had an average of only 0.11 ng L^{-1}.

3.7 PFASs leaching from the landfill

In area A, the leaching through the remaining open part of the old landfill at L1 was estimated with ∑PFASs 26 mg d^{-1} with the main contributors of PFCAs with 15 mg d^{-1} (57% of ∑PFASs) and PFSAs with 9.6 mg d^{-1} (37% of ∑PFASs). The dominating single substances was PFOS with 7.02 mg d^{-1} (27%, linear and branched isomers combined) and PFOA with 5.7 and mg d^{-1} (22%). Sample L2 at the old landfill showed a daily average leaching of ∑PFASs with 9.6 mg d^{-1}. Dominating substances were PFBS with 3.6 mg d^{-1} (37% of ∑PFASs and 94% ∑PFSAs), PFHxA with 2.9 mg d^{-1} (30% ∑PFASs and 65% ∑PFCAs) and 6:2 FTSA with 1.3 mg d^{-1} (14% ∑PFASs and 93% ∑FTSAs). In area A on the active landfill at L4, the leaching of ∑PFASs was estimated with 104 mg d^{-1}. PFCAs were representing the largest contributor with 66 mg d^{-1} (62% of ∑PFASs), followed by PFSAs with 32 mg d^{-1} (31% of ∑PFASs) and precursors with 6.6 mg d^{-1} (6.3 of ∑PFASs). PFOA with 27 mg d^{-1} (26% of ∑PFASs) and PFHxA with 17 mg d^{-1} (16% of ∑PFASs) were the most abundant compounds of PFCAs. For PFSAs, PFOS contributed the most with 17 mg d^{-1} (sum of linear and branched PFOS, 16% of ∑PFASs). Sampling location L5 represent the whole area A with an estimated leaching of 540 mg d^{-1} for ∑PFASs. The most abundant class were PFCAs with 360 mg d^{-1} (67%) followed by PFSAs with 130 mg d^{-1} (24%) and precursors with 45 mg d^{-1} (8.3%). Most contributing single substances were PFOA (140 mg d^{-1}, 26%), followed by PFHxA (86 mg d^{-1}, 16%) and PFBA (70 mg d^{-1}, 13%. For PFSAs, PFBS contributed the most with 43 mg d^{-1} (8.0%) and 6:2 FTSA with 22 mg d^{-1} (4.09%) was the most abundant compound among the precursors.

In area B, the leaching from soil cell L6 was estimated with 4.7 mg d^{-1} for ∑PFASs. PFCAs were the most abundant class with 2.5 mg d^{-1} (52%), followed by PFSAs with 1.4 mg d^{-1} (30%) and FTSAs with 0.86 mg d^{-1} (18%). PFOA (1.2 mg d^{-1}, 25% of the

$\sum$PFASs) and PFHxA (0.75 mg d^{-1}, 16%) were the most abundant compounds among the PFCAs. PFOS (0.75 mg d^{-1}, 16%) and PFHxS (0.35 mg d^{-1}, 8.7%) were measured with the highest contribution for PFSAs. 6:2 FTSA was the most abundant compound among the precursors (0.7 mg d^{-1}, 15% of the $\sum$PFASs). The leaching from the sludge cell L7, was calculated with 22 mg d^{-1} for the $\sum$PFASs. Precursors were the most contributing class with 17 mg d^{-1} (76%), followed by PFCAs 4.1 mg d^{-1} (19%) and PFSAs 1.06 mg d^{-1} (5%). Most contributing single substances were 6:2 FTSA (16 mg d^{-1}, 72% of $\sum$PFASs), PFHxA (3.08 mg d^{-1}, 14% $\sum$PFASs) and 8:2 FTSA (0.902 mg d^{-1}, 4.1% of $\sum$PFASs). At L12, the sampling location for the whole area B, a total $\sum$PFASs leaching of 41 mg d^{-1} was estimated, composed of 46% PFCAs, 39% PFSAs and 15% FTCAs. PFOS combined for the linear and the branched isomer was the most abundant compound (12 mg d^{-1}, 29% of the $\sum$PFASs), followed by 6:2 FTSA (11 mg d^{-1}, 28% $\sum$PFASs). PFHxA (4.1 mg d^{-1}, 10% of $\sum$PFASs) and PFBA (3.3 mg d^{-1}, 8% $\sum$PFASs) were the most abundant compounds among the PFCAs. At W1, the inflow to the WWTP, a $\sum$PFASs leaching of 410 mg d^{-1} was estimated. PFCAs were the largest contributor with 64%, followed by PFSAs (30%) and FTCAs (6%). PFOA (86 mg d^{-1}, 21% $\sum$PFASs) and PFHxA (80 mg d^{-1}, 19% $\sum$PFASs) contributed most for the PFCAs. PFOS (sum of linear and branched, 13% $\sum$PFASs), PFHxS (sum of linear and branched, 9% $\sum$PFASs) and PFBS (8.5% $\sum$PFASs), made up a leaching 53.3 mg d^{-1}, 37 mg d^{-1} and 35 mg d^{-1} respectively. The Leaching at the outflow of the landfill at W9 was calculated with 220 mg d^{-1}, of which 74% were PFCAs, 24% PFSAs and 2% FTSAs. PFHxA was the most abundant compound (6.6 mg d^{-1}, 30% $\sum$PFASs), followed by PFBA, (3.9 mg d^{-1}, 18% $\sum$PFASs), PFPeA (2.2 mg d^{-1}, 10% $\sum$PFASs) and PFOA (2.2 mg d^{-1}, 10% $\sum$PFASs). PFBS was the most abundant among the PFSAs (30.8 mg d^{-1}, 14% $\sum$PFASs).

3.8 Mass flow in the river

The mass flow of PFASs in the river is presented in figure 3.8. The first sample at R0 showed a mass flow $\sum$PFASs of 8.1 mg d^{-1}. Only PFCAs (59%) and PFSAs (41%) were present in this sample. Most abundant compounds were PFHpA (55% of $\sum$PFASs), PFHxS (27% of $\sum$PFASs) and PFOS (14% of $\sum$PFASs). At R1 a mass flow for $\sum$PFASs of 180 mg d^{-1} was calculated. PFCAs were the most abundant class present with 62%, followed by PFSAs (35%) and FTCAs (3%). Most abundant compounds were PFOA (21%), PFHxA

(19%), PFBA (14%) and PFHpA (7.8%) for PFCAs, PFHxS (16%), PFOS (12%) and PFBS (6.4%) for PFSAs and Et-FOSAA (2.7%) for the precursors.

At R3 (1400 mg d^{-1} of $\sum$PFASs), PFCAs were the dominating class (67%) with PFSAs covering the remaining 33%. Most abundant compounds were PFHxA (27%), PFOA (17%) and PFBA (16%) among the PFCAs and PFHxS (16%), PFBS (12%) and PFOS (5.5%) among the PFSAs. In the samples R4-R11, PFSAs were the dominating class averaging 94% of $\sum$PFASs. The dominating single substances were PFHxS (45%) and PFOS (44%). After the inflow of the water exiting the landfill (R2) the mass flow increased to 2070 mg d^{-1}. Afterwards, the concentration continuously decreased up to R6 (120 mg d^{-1}). In the following the mass flow continuously increased again until lake Ekoln (10000 mg d^{-1}). However, in the Fyrisån (R9), the mass flow increased fourfold to 8100 mg d^{-1} compared to the exit of the Sävjaån at R8.

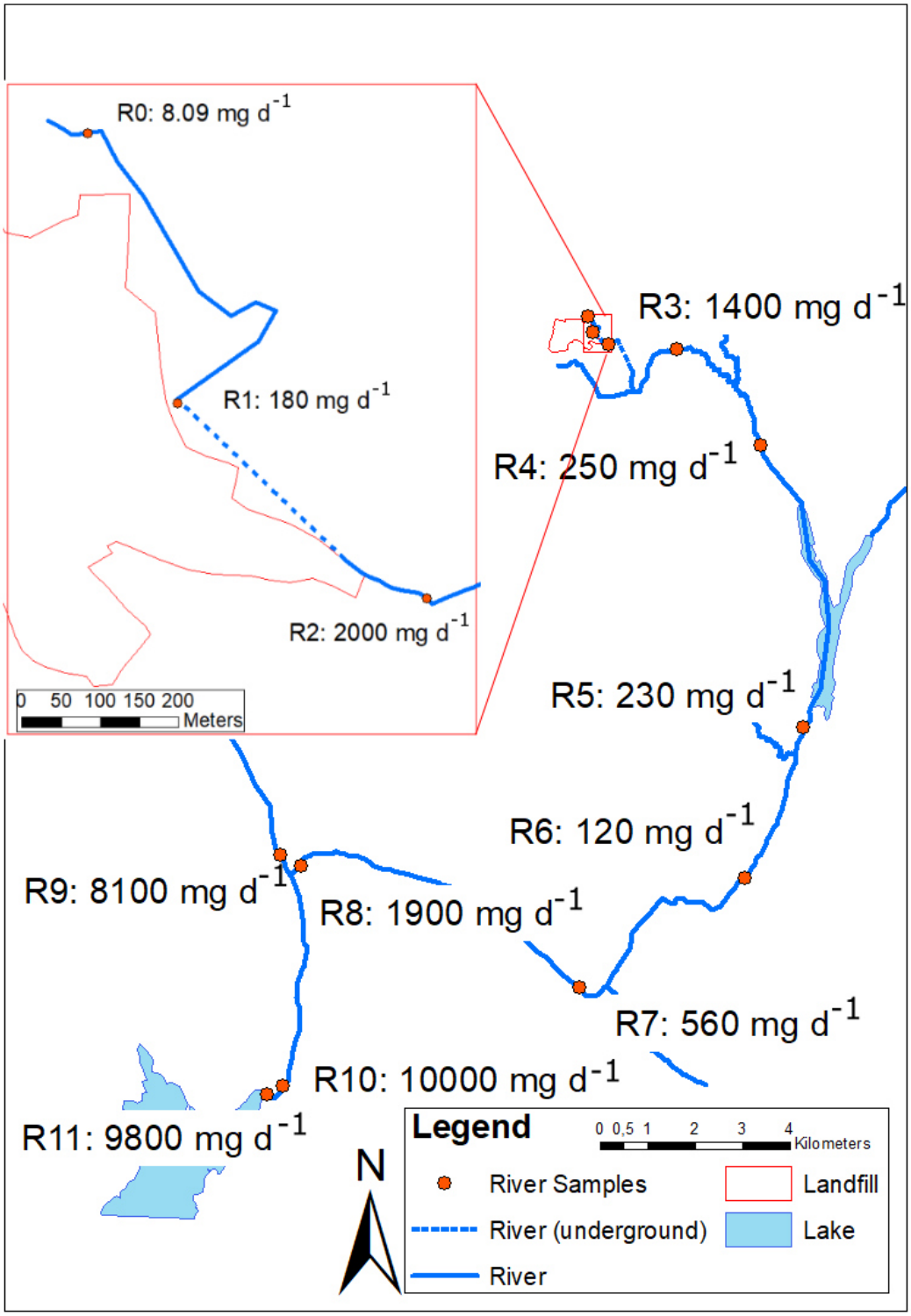

Figure 3.8: Mass flow in the river

4 Discussion

4.1 PFAS concentration at the landfill and the nearby groundwater

The $\sum$PFAS concentrations in the landfill leachate and drainage system at the landfill site were generally larger in area A (980 ng L^{-1}, L1-L5) compared to area B (490 ng L^{-1}, L6-L12). The difference in concentration must be related to the kind of waste deposited in the different area. The lower concentration in area B might be related to the fact that soil and sludge is only temporarily stored in the corresponding cells, while area A (old and active landfill) represent a permanent storage of waste. In fact, both soil and sludge from area B will eventually be stored in area A. Another reason for the higher concentration could be the larger amount of refuse that is deposited in area A. However, the concentrations for L2 and L3 in area A require some additional explanation, as they do not fit into the overall picture. The concentration at L2 (450 ng L^{-1}) is very likely to be related to the sludge which is built into the landfill sealing. As described later, sludge contains considerable amounts of PFASs which are prone to leaching out of the sealing, especially considering that drainage water will quickly percolate through the material on top of the impermeable layer (150 cm). Sampling site L3 (59 ng L^{-1}) stands out because of the very low concentration, especially since the neighbouring sampling site L4 (both located on the active landfill) shows a 22 times higher concentration (1300 ng L^{-1}). The sampling of the locations of L3 and L4 was conducted via tubes reaching down to the drainage system. At sampling location L4, the sampling depth was between 17 and 18 m, whereas the sampling depth at L3 was only between 12 and 13 m. At L4, the sampling equipment clearly reached the bottom of the surface drainage, whereas at L3 the equipment only penetrated through a water surface. Thus, sample L3 represent standing water and was not actively in contact with the landfill leachate. It is therefore assumed that the

water sampled at L3 was no drainage water but precipitation water gathering in the tube. This has been confirmed by observable damage to the drainage system around the active landfill. Typical concentration of PFASs in precipitation are ranging from 0.91 ng L^{-1} to 13 ng L^{-1} (Kim and Kannan, 2007) or 1.4 ng L^{-1} to 19 ng L^{-1} ($\sum$PFCAs) (Kwok et al., 2010). which is considerably lower than measured at the landfill. The increase in concentration comparing site L4 and L5 seems reasonable, since all sections from area A are combined at this point. The highest concentration at site L7 (880 ng L^{-1}) in area B is related to the sludge deposed in the cell. Sludge is deposited in the cell every month, thereby PFASs can constantly leach out from the sludge. The decrease in concentration in the nearby site L8, where the drainage systems from the soil cell and the sludge cell are united, might be related to the lower concentration in the leachate of the soil cell by having an almost equal flow, since the areas of both cells show almost the same size. Further PFASs inputs leading to an overall increase in concentration at L12 which can be related to the basins where sludge from the STP on the site and municipal sewage system of Uppsala is dumped and can leach into the drainage.

The composition profile in area A is clearly dominated by PFCAs (62% $\sum$PFASs). Short-chain compounds ($C_3 - C_6$) and PFOA (C_7) account for 98% $\sum$PFCAs indicating that compounds with chain lengths of C_8 and longer are hardly present in the liquid phase. For area A, only in sample L1 compounds with chains longer C_{10} and longer have been detected. For PFSAs (29% $\sum$PFASs), the short chain compound PFBS was the highest contributing single substance (34% $\sum$PFSAs) when the branched and linear isomers of PFOS are considered separately ($\sum$PFOS 44% $\sum$PFSAs). For area B, the dominant group of substance are FTSAs (42% $\sum$PFASs) followed by PFCAs (35%) and PFSAs (19%). This shift in composition is likely to be referred to the sludge deposition at several places in area B thereby influencing the composition of the drainage water, which will be discussed later on. Both, the preference of shorter-chain compounds over their long-chain counterparts and the dominace of PFCAs in the landfill leachate over PFSAs can be explained by differences in sorption behaviour between both the chain length as wells as the carboxylic and sulfonic head groups (Higgins and Luthy, 2006). They have shown that increasing chain length is positively correlated to increasing values in the distribution coefficient (log K_d), supporting the enrichment of long-chain isomers in organic-matter fractions. Therefore, the shorter the perflouoralkyl chain, the stronger the partitioning into the liquid phase. As shown above, this picture is visible in the findings in this study. Higgins and Luthy (2006) investigated in the same study differences between the head

groups. They found that the sulfonic head group (i.e. PFSAs) has a stronger adsorption potential than the carboxylic group (i.e. PFCAs). This effect is also in agreement with the findings in this study. The average concentration for PFCAs (52%) was almost twice as high as for PFSAs (27%) in the landfill leachate.

In recent years, a number of studies have shown, similar findings (Benskin et al., 2012; Busch et al., 2010; Fuertes et al., 2017; Huset et al., 2011; Li et al., 2012). Benskin et al. (2012) found generally higher contributions of PFCAs (16-56% $\sum$PFASs) compared to PFSAs (12-21%) in landfill leachates. In this study PFCAs accounted for 52% $\sum$PFASs and PFSAs for 27%. Benskin et al. (2012) have furthermore shown that PFPeA (570-1800 ng/L) and PFHxA (670-2500 ng L^{-1}), both short-chain PFCAs, were the dominating compounds. In this study, PFPeA (29 ng L^{-1}) and PFHxA (120 ng L^{-1}) were not the most abundant compounds, but very frequently detected (79% and 100% respectively). Li et al. (2012) found PFCAs as the major contributing class of compounds (73%), suggesting that the abundancy is related to the degradation of fluorotelomer and perfluoroalkyl sulfonyl products. They found PFHxA as the most dominant single substance (25% $\sum$PFASs). PFHxA in this study only accounted for 4.1% $\sum$PFASs. The three major contributors of the PFCAs (PFBA 27% $\sum$PFASs, PFHxA 15% and PFOA 12%) in the study of Busch et al. (2010) were also the three major constituents of the leachate in this study (PFBA 8.06% $\sum$PFASs, PFHxA 16%, PFOA 18%). Eggen et al. (2010) found PFHxA (12% $\sum$PFASs) and PFOA (13%) as the main contributors among the PFCAs. In general, overall PFASs distribution shows a similar pattern. PFCAs are more abundant in landfill leachates than PFSAs and also the composition profiles show that especially PFCAs ($C_3 - C_8$) are more frequently detected and in larger quantities.

One major difference in the landfill leachate, however, were the $\sum$PFASs concentration. In this study, the highest measured concentration measured 1800 ng L^{-1}. This value was far lower than findings in other studies. For instance, Eggen et al. (2010) detected 6123 ng L^{-1} for $\sum$28PFASs in Norway. Busch et al. (2010) detected up tp 12819 ng L^{-1} for $\sum$43PFASs in 22 landfill sites in Germany. In a study performed in Canada, Li et al. (2012) found concentrations up to 21300 ng L^{-1} $\sum$13PFASs. Yan et al. (2015) found concentrations of 292000 ng L^{-1} $\sum$14PFAS in China. The findings from Fuertes et al. (2017) were closer to the findings in this study. They found a $\sum$16PFAS concentration of 1380 ng L^{-1} in untreated leachate and 3160 ng L^{-1} in Spain. This large difference in concentration is probably because of i) type of waste deposited as well as the amount (Benskin et al., 2012),

ii) refuse from manufacturing facilities are prone to contain much higher concentrations than those landfills which are not associated with this sort of waste (Yan et al., 2015), and iii) time period of usage (or closed) of the landfill (Busch et al., 2010). In this case study at Hovgården, there is obviously no direct waste disposal from fluorochemical manufacturing or fluorochemical application processes. One major medium that is deposed at Hovgården are ashes. These ashes come from incineration plants producing energy by burning MSW. According to the operating temperature and the efficiency of the incineration process, most PFASs within the MSW will be destroyed (Busch et al., 2010). Thus, the ashes should theoretically not contain high PFAS concentrations anymore. This hypothesis is above was confirmed by the study of Busch et al. (2010), who detected effective destruction of FTBP composites forming hydrogen fluoride during the combustion process.

The $\sum$PFAS concentration for the groundwater sample G9.2 certainly stands out (1800 $\mathrm{ng\,L^{-1}}$) which was the highest measured PFAS concentration of all samples. The damage in the drainage system underneath the active landfill as well as the groundwater flow direction might be related to the high concentration at G9.2. The leachate from the active landfill will drain towards G9.2 before the vertical barrier will prevent further flow into the direction of the groundwater flow (east). From there the water will percolate back into the direction of the drainage system. It can be assumed that the leakage in the drainage system allows the PFASs to be translocated until G9.2 where they can accumulate. Similarly, the second highest $\sum$PFASs concentration in the groundwater was identified at site G9.1 $\mathrm{ng\,L^{-1}}$). It is possible that G9.1 (8.1m depth) is influenced by G9.2 (8m depth), especially since these two wells are located just a few cm apart from each other. This assumption, of course, would suggest a leakage through the vertical barrier. It is unclear how effectively the vertical barrier is working. For some of the remaining wells, G6 ($\sum$PFAS concentration = 460 $\mathrm{ng\,L^{-1}}$) as well as G7 (96 $\mathrm{ng\,L^{-1}}$) and G8 (290 $\mathrm{ng\,L^{-1}}$) are situated closely together. They might be affected by the sludge drainage but there is no clear evidence. The wells located around the old landfill (i.e. G1, G2 and G3) are likely to be influence by the old landfill. G2 (340 $\mathrm{ng\,L^{-1}}$) and G3 (309 $\mathrm{ng\,L^{-1}}$) showed similar concentrations which are located in the main direction of the groundwater flow (i.e. southwestern), as the concentration in G1 is considerably higher (85 $\mathrm{ng\,L^{-1}}$). G4 ($\sum$PFAS concentration = 42 $\mathrm{ng\,L^{-1}}$) and G5 (8.5 $\mathrm{ng\,L^{-1}}$) are the only representative reference samples, which are supposed to be no influenced by the landfill leachate. These are also the only two groundwater sampling locations that are below the threshold for PFASs concentration by the Swedish Geological Institute of 45 $\mathrm{ng\,L^{-1}}$ (Banzhaf et al., 2017). In

general, the $\sum$PFAS concentrations showed a high variability between the samples (8.5-1800 ng L^{-1}) as well as the PFAS composition profile (Figure 3.1), which can be related to the differences in sampling site conditions such as the sampling depth. Hydrogeological conditions such as the direction of groundwater flow can also support the heterogenic distribution of PFASs in the groundwater at Hovgården.

The composition profile of the groundwater is dominated by PFCAs (60% $\sum$PFASs). PFSAs contribute with 37% $\sum$PFASs, whereas precursor compounds only hold for 2% $\sum$PFASs. PFCAs with shorter chainlength ($C_3 - C_7$) account for 99% of the $\sum$PFCAs. For PFSAs, shorter chains ($C_4 - C_6$) account for 81% $\sum$PFSAs. This clearly indicated that compounds with shorter chain lengths are clearly dominating the composition profiles of groundwater. Short-chain PFASs interact less strongly with organic fractions or mineral surfaces, supporting their mobility and translocation by percolating water into deeper soil horizons and increasing their leaching potential (Sepulvado et al., 2011). As described above, sulfonic head groups showed stronger adsorption potential to solid phases compared to carboxylic head groups, supporting the higher abundancy of PFCAs in the groundwater than PFSAs (Higgins and Luthy, 2006). Interestingly, PFOA is the most abundant compound in the groundwater. According to Higgins and Luthy (2006) and Enevoldsen and Juhler (2010), one would expect the compound with the shortest chain length (PFBA) to be more abundant as the hydrophobicity increases with increasing chain length. The study by Eschauzier et al. (2013) investigated the groundwater situation concerning PFASs in the Netherlands and they also found that PFOA is more abundant than shorter chain compounds (PFBA, PFHxA and PFHpA). They related this finding to the larger production volumes of PFOA compared to PFBA. However, with increasing distance to the source, the composition profile of the groundwater shifted towards PFBA as the dominating compound (Eschauzier et al., 2013). This indicated that the composition of the origin of the PFASs plays the major role close to the source, but that mobility plays the major role with increasing distance from the source. Considering that the sampling depths of the groundwater was considerably lower (max. 8.1 m) than in the study by Eschauzier et al. (2013) (min. 25 m) this effect might be even more pronounced in the present study. The $\sum$PFAS concentrations in the study by Eschauzier et al. (2013) (4.2-4400 ng L^{-1}) ranked in the same range as the present study (8.5-1800 ng L^{-1}). The sampling design however, does not coincide. The sampling in the present study was spread out on and around the landfill area, whereas Eschauzier et al. (2013) sampled several groundwater depths.

Factors controlling the mobility of PFASs in soil or other solid material are, among others, the ionic strength and pH. Wang et al. (2012) and Wang and Shih (2011) have investigated sorption and desorption processes of PFOS and PFOA on mineral surface boehmite and alumina. These studies revealed that interactions between positively charged mineral surfaces and negatively charged PFASs is influenced by the ionic strength. Increasing ionic strength caused desorption of PFASs as electrostatic attraction was reduced. Furthermore, chloride anions more strongly competed for the available surface sites, leading to desorption of PFASs form the mineral surface. Another factor influencing the PFASs concentration in the leachate is the pH. Benskin et al. (2012) found that PFAS become more mobile with increasing pH. The pH can either ionize the PFASs or change the electrostatic behaviour of the sorbent (Higgins and Luthy, 2006). The pH has not been measured in this study but in environmental matrices it is usually above the pKa values for most PFASs which is why the latter mechanism seems to be more likely (Benskin et al., 2012). Increasing pH might lead to protonation of solid phase surfaces, reducing the number of available sites on the sorbent. At the pH of sludge, PFASs are deprotonated and in their anionic form. The negatively charged organic matter/sludge surface and the anionic PFASs would therefore repel each other electrostatically. There exists a possibility that Ca and Mg ions enable electrostatic interactions through bridge bonds. At lower pH, the concentration of positive charges on the sludge surface increases, favouring the interaction with the anionic PFASs (Milinovic et al., 2016).

The $\sum$PFAS concentration in the sludge (33-440 ng $g_{dw}{}^{-1}$) does not show a homogenous picture. It seems that the concentrations in the winter months are lower (33.77 ng $g_{dw}{}^{-1}$) than in the summer and autumn (190-440 ng $g_{dw}{}^{-1}$). However, this is only speculation since there is no data available for every month throughout the course of a whole year. The composition profile of the sludge is dominated by precursor compounds (59% $\sum$PFASs). The most abundant group is represented by FTSAs (37% $\sum$PFASs). PFSAs (33%) are the second most abundant group of substances, PFCAs (7.6%) are the least abundant group. Among the PFCAs, however, the composition differed remarkably from the liquid samples (leachate and groundwater). PFCAs with shorter chain length ($C_5 - C_8$) accounted for only 2.7% of the $\sum$PFASs with PFBA and PFPeA being completely absent. Longer chain PFCAs ($C_8 - C_{14}, C_{16}, C_{18}$) were present. Except PFOcDA (33% detection frequency), every substance ($C_8 - C_{14}, C_{16}, C_{18}$) has been detected with a frequency of 100% (4.8% $\sum$PFASs). In the case of PFSAs, the long-chain compound PFOS is the most abundant compound (30% $\sum$PFASs and 91% $\sum$PFSAs). This composition can be explained by

same arguments used to explain the composition of the liquid (leachate and groundwater samples). As compounds with longer chain lengths have a larger tendency to accumulate on solid surfaces than their-short chain counterparts, they will be enriched in solid phases, especially on organic matter (Enevoldsen and Juhler, 2010; Higgins and Luthy, 2006). Sewage sludge with relatively high organic carbon content may therefore be a suitable medium for long-chain PFASs to accumulate (Johnson et al., 2007). Also, the differences in sorption behaviour between carboxylic and sulfonic head groups are noticeable. The presence of precursors in the sludge, such as 6:2 FTSA has been found by Wang et al. (2011). They suggest that the enrichment of 6:2 FTSA is associated with the formation of strong covalently bound complexes between 6:2 FTSA and organic components in the sludge. The porosity of the sludge further promotes the accessibility of surface sites on which the sorption of PFASs can take place (Ochoa-Herrera and Sierra-Alvarez, 2008; **?**). The presence of PFAS precursor in sludge has been detected in previous studies. Sepulvado et al. (2011) and Higgins et al. (2005) found FOSAA, Me-FOSAA and Et-FOSAA. These substances have been found to be formed as products of biotransformation processes of for example Me-FOSE and Et-FOSE(Huset et al., 2011), which were not present in the sludge in this study. PFAS precursors such as FOSAAs, however, are no stable end products but undergo further degradations processes to form stable end products such as PFSAs (Rhoads et al., 2008). It has been proposed a transformation pathway of Et-FOSE being transformed to the stable end product PFOS in activated sludge with several intermediate products such as Et-FOSAA and FOSA (Rhoads et al., 2008). In this study, both Et-FOSAA and FOSA were detected in the sludge samples with a composition of 4.8% and 15% of the $\sum$PFASs.

4.2 PFASs in the STP and removal efficiency

The removal of PFASs in this treatment system is likely related to sorption of PFASs to particles and subsequent sedimentation, as there is no advanced tertiary treatment step implemented into the treatment process. The removed PFASs in the first aeration step (36%) and in the sedimentation pond after the MBBR treatment (42%) could be explained by sorption processes (Campo et al., 2014). As explained above, long-chain PFCAs and PFSAs have been found to more preferably partition into the solid phase (sludge) (Higgins and Luthy, 2006). This can be confirmed by comparing the composition profile of the

sludge investigated in this study and the removed PFASs within the STP. Figure 3.5 clearly shows this trend. The most efficiently removed PFASs in the STP were long-chain $C_8 - C_{14}; C_{16}, C_{18}$ PFCAs (total removal 88% (PFNA) and 100% (PFDA)) and C_6, C_8 PFSAs (total removal 56% (PFHxS linear), 42% (PFHxS branched), 90% (PFOS linear) and 84% (PFOS branched)), FTSAs (total removal 77% (6:2 FTSA) and 100% (8:2 FTSA)), FOSA (total removal 53% (FOSA linear) and 66% (FOSA branched)) and FOSAAs (total removal 100% for both Me- and Et-FOSAA). These PFASs were also the most abundant in the sludge, strongly suggesting sorption of PFASs in the treatment system. For the precursor compounds in the present study 8:2 FTSA, Me-FOSAA and Et-FOSAA the removal in the STP has been very efficient with 100% removal. On the one hand, this can again be related to sorption processes (Higgins et al., 2005; Wang et al., 2011) or to transformation due to biodegradation. As discussed for the sludge above, FOSAAs can undergo biological transformation forming PFOS (Higgins et al., 2005; Rhoads et al., 2008). Zhang et al. (2016) suggest for 6:2 FTSA to be aerobically transformed mainly to short-chain PFCAs, such as PFPeA and PFHxA. Beside sorption and degradation, atmospheric release could be a third option for decreasing concentrations in sewage treatment processes which has been shown for WWTPs and landfills Ahrens et al. (2011). The negative removal efficiency in the polishing ponds could be related to sampling errors, matrix effects, atmospheric deposition or additional sources within the system (degradation) (Campo et al., 2014). Schultz et al. (2006) also found negative removal efficiencies but suggested degradation of precursors during activated sludge processes as the reason for it. As the negative removal efficiency in this study did not occur during this treatment process, it might be rather related to desorption processes. (Negative removal efficiencies have been reported before (Arvaniti et al., 2012; Campo et al., 2014; Schultz et al., 2006) Campo et al. (2014) found negative removal efficiency of -577% only for PFNA and Arvaniti et al. (2012) Arvaniti et al. 2012 found negative removal efficiency for PFOS of -408%.

4.3 Mass fluxes and transport into the environment

The calculations concerning the leaching of PFASs from the landfill are rough estimations. The calculations are based on the precipitation amount using daily mean precipitation data collected on Hovgården over a period of one year and PFASs concentration in the leachate collected in February and March, 2017. The uncertainty in the calculation would

have been lower of more parameters influencing the infiltration and percolation behaviour were included. In general, the highest leaching came from area A (540 $\mathrm{mg\,d^{-1}}$) which is due to the two large deposition sites (old and active landfill), and the large amount of precipitation going down on this part. The contribution of area B (41 $\mathrm{mg\,d^{-1}}$) does not contribute as much, most likely due to the temporary storage of both soil and sludge in area B. During the treatment process the mass flow of PFASs decreased from 412 $\mathrm{mg\,d^{-1}}$ to 220 $\mathrm{mg\,d^{-1}}$. It is likely that at least parts of the flow enter the groundwater, especially since there were elevated PFAS concentration in the PFASs concentrations of groundwater sites (G9.1, G9.2, G6). The permanent storage of refuse on area A represent a large PFASs leaching potential. As there is no unbroken record since the beginning of the landfill, and therefore only sketchy documentation of the refuse stored on Hovgården, it would be speculative to assert what is directly responsible as a source.

In the river at site R0, the $\sum$PFAS concentration was low (1.8 $\mathrm{ng\,L^{-1}}$) which can be explained by the fact that this concentration is just a background contamination and is not attributable to contamination from the landfill. Surprisingly, the following sampling location R1, reveals the highest $\sum$PFAS concentration of all river samples (41 $\mathrm{ng\,L^{-1}}$), with the exception of R2 as explained above, although the water flowing out of the landfill has not even entered. Sampling site R1 is very closely located to the landfill and relocation of the stream underground, which may have had influenced site R1. At R2, shortly after the inflow of the water from the landfill, the concentration increased (440 $\mathrm{ng\,L^{-1}}$). The decrease in concentration between R2 and R3 (29 $\mathrm{ng\,L^{-1}}$) is large. It is questionable where the PFASs flow to. Leaching to the groundwater is unlikely since the underground section between R2 and R3 is running in pipes. It is possible that the stream entering the observed river has some dilution effects, considering that it is not affected by PFASs. Sampling in this stream has not been done, however, if it is the case, it would be an indication for Hovgården not having an effect on the surroundings into the western and southern direction, since this stream is running on the western and southern border. The concentrations decrease until R6 (0.3 $\mathrm{ng\,L^{-1}}$). The increase in R7 (0.96 $\mathrm{ng\,L^{-1}}$) could be related to another inflow between R6 and R7 from the southeastern direction. The further increase at R8 (3.3 $\mathrm{ng\,L^{-1}}$) might be due to the fire-fighting training facilities at Viktoria, Uppsala. At R9 (7.9 $\mathrm{ng\,L^{-1}}$) in the Fyrisån and the following sample R10 (6.2 $\mathrm{ng\,L^{-1}}$) and R11 (6.02 $\mathrm{ng\,L^{-1}}$) are very likely related to PFAS contamination further upstream. A WWTP (Kungsängsverket) approximately 2 km upstream could be a point source for PFASs. However, Gago-Ferrero et al. (2017) found that in this particular case this WWTP

does not have such a big influence concerning the PFASs input. (Gago-Ferrero et al., 2017) suggest, that the PFASs contamination is more likely to be related to other small scale on-site treatment facilities further upstream.

The mass flow of PFASs in the river (Figure 3.8), follows the same pattern as the concentrations. The decrease after the inflow of the water from the landfill (R2) the mass flow constantly decreases up to (R6). This is firstly due to the increasing volume in the rivers and secondly due to no further PFAS input from inflowing streams. At R7 the mass flow increases fourfold. As mentioned above it is possible that the inflowing stream is responsible for input of PFASs. In the Fyrisån the effects mentioned above as well as the larger flow rate are responsible for the increase in PFAS mass flow.

5 Conclusion and future perspectives

From the investigations in this study can be concluded that Hovgården landfill is a source for PFASs to the environment. The composition profile for the leachate and also the groundwater are in line with previous studies as discussed above. The general pattern of short-chain PFCAs and PFSAs dominating over their long-chain counterparts is clearly visible. As well in line with previous findings is the composition profile of the sludge which is, opposite to the liquid samples, not dominated by PFCAs but PFSAs and precursors. The shift to more abundant long-chain compounds represents their affinity to sorb to solid phases. This effect was also found in the STP where long-chain compounds and precursors were very efficiently removed. The overall removal efficiency is surprisingly high, considering the simple treatment steps implemented on Hovgården. In this concern however, it might be worth considering expanding the STP to further improve the removal efficiency. This might not only be interesting with respect to PFASs but also other contaminants which for sure are present in the leachate as well. The mass flow estimations have shown that a long-distance effect for surface waters emerging from Hovgården is not expected. The local effects nearby the landfill however should not be underestimated. Groundwater systems might eventually be affected, especially since there is no constructed underground sealing. Migration processes into the groundwater and translocation processes within aquifers are slow processes. PFASs however are extremely persistent and do not degrade. In the long run, this could cause some issues if the PFASs from Hovgården migrate into regions of drinking water wells. Gyllenhammar et al. (2015) have shown such a case for Uppsala. Most of the groundwater concentrations were above the threshold for groundwater for PFOS (45 $\mathrm{ng\,L^{-1}}$) and also above the threshold for drinking water for $\sum_{11}$PFASs (90 $\mathrm{ng\,L^{-1}}$). It is only speculation, but Uppsala is expanding, especially in the north-eastern area of Granby. If in the future new drinking water resources have to be made accessible, the nearby landfill and the effects related to PFASs should be considered. For Hovgården it would therefore be beneficial if all of the leachate is collected and treated.

In combination with the right treatment measures, this could minimize the risk. As any other landfill, also Hovgården represents a long-term source, suggesting that improvements for the leachate treatment will also pay off in the long run.

Bibliography

Ahrens, L., Shoeib, M., Harner, T., Lee, S. C., Guo, R., and Reiner, E. J. (2011). Wastewater Treatment Plant and Landfills as Sources of Polyfluoroalkyl Compounds to the Atmosphere. *ENVIRONMENTAL SCIENCE & TECHNOLOGY*, 45(19):8098–8105.

Allred, B. M., Lang, J. R., Barlaz, M. A., and Field, J. A. (2015). Physical and Biological Release of Poly- and Perfluoroalkyl Substances (PFASs) from Municipal Solid Waste in Anaerobic Model Landfill Reactors. *ENVIRONMENTAL SCIENCE & TECHNOLOGY*, 49(13):7648–7656.

Arvaniti, O. S., Ventouri, E. I., Stasinakis, A. S., and Thomaidis, N. S. (2012). Occurrence of different classes of perfluorinated compounds in Greek wastewater treatment plants and determination of their solid-water distribution coefficients. *JOURNAL OF HAZARDOUS MATERIALS*, 239:24–31.

Banzhaf, S., Filipovic, M., Lewis, J., Sparrenbom, C. J., and Barthel, R. (2017). A review of contamination of surface-, ground-, and drinking water in Sweden by perfluoroalkyl and polyfluoroalkyl substances (PFASs). *AMBIO*, 46(3):335–346.

Benskin, J. P., Li, B., Ikonomou, M. G., Grace, J. R., and Li, L. Y. (2012). Per- and Polyfluoroalkyl Substances in Landfill Leachate: Patterns, Time Trends, and Sources. *ENVIRONMENTAL SCIENCE & TECHNOLOGY*, 46(21):11532–11540.

Buck, R. C., Franklin, J., Berger, U., Conder, J. M., Cousins, I. T., de Voogt, P., Jensen, A. A., Kannan, K., Mabury, S. A., and van Leeuwen, S. P. J. (2011). Perfluoroalkyl and polyfluoroalkyl substances in the environment: Terminology, classification, and origins. *Integrated environmental assessment and management*, 7(4):513–541.

Busch, J., Ahrens, L., Xie, Z., Sturm, R., and Ebinghaus, R. (2010). Polyfluoroalkyl compounds in the East Greenland Arctic Ocean. *JOURNAL OF ENVIRONMENTAL MONITORING*, 12(6):1242–1246.

Campo, J., Masia, A., Pico, Y., Farre, M., and Barcelo, D. (2014). Distribution and fate of perfluoroalkyl substances in Mediterranean Spanish sewage treatment plants. *SCIENCE OF THE TOTAL ENVIRONMENT*, 472:912–922.

de Voogt, P. and Saez, M. (2006). Analytical chemistry of perfluoroalkylated substances. *TRAC-TRENDS IN ANALYTICAL CHEMISTRY*, 25(4):326–342.

Eggen, T., Moeder, M., and Arukwe, A. (2010). Municipal landfill leachates: A significant source for new and emerging pollutants. *SCIENCE OF THE TOTAL ENVIRONMENT*, 408(21):5147–5157.

Enevoldsen, R. and Juhler, R. K. (2010). Perfluorinated compounds (PFCs) in groundwater and aqueous soil extracts: using inline SPE-LC-MS/MS for screening and sorption characterisation of perfluorooctane sulphonate and related compounds. *ANALYTICAL AND BIOANALYTICAL CHEMISTRY*, 398(3):1161–1172. 6th Annual LC/MS/MS Workshop on Environmental Applications and Food Safety, Barcelona, SPAIN, FEB 25-26, 2010.

Eschauzier, C., Raat, K. J., Stuyfzand, P. J., and De Voogt, P. (2013). Perfluorinated alkylated acids in groundwater and drinking water: Identification, origin and mobility. *SCIENCE OF THE TOTAL ENVIRONMENT*, 458:477–485.

Fuertes, I., Gomez-Lavin, S., Elizalde, M. P., and Urtiaga, A. (2017). Perfluorinated alkyl substances (PFASs) in northern Spain municipal solid waste landfill leachates. *CHEMOSPHERE*, 168:399–407.

Gago-Ferrero, P., Gros, M., Ahrens, L., and Wiberg, K. (2017). Impact of on-site, small and large scale wastewater treatment facilities on levels and fate of pharmaceuticals, personal care products, artificial sweeteners, pesticides, and perfluoroalkyl substances in recipient waters. *SCIENCE OF THE TOTAL ENVIRONMENT*, 601:1289–1297.

Gyllenhammar, I., Berger, U., Sundstrom, M., McCleaf, P., Euren, K., Eriksson, S., Ahlgren, S., Lignell, S., Aune, M., Kotova, N., and Glynn, A. (2015). Influence

of contaminated drinking water on perfluoroalkyl acid levels in human serum - A case study from Uppsala, Sweden. *ENVIRONMENTAL RESEARCH*, 140:673–683.

Higgins, C., Field, J., Criddle, C., and Luthy, R. (2005). Quantitative determination of perfluorochemicals in sediments and domestic sludge. *ENVIRONMENTAL SCIENCE & TECHNOLOGY*, 39(11):3946–3956.

Higgins, C. P. and Luthy, R. G. (2006). Sorption of perfluorinated surfactants on sediments. *ENVIRONMENTAL SCIENCE & TECHNOLOGY*, 40(23):7251–7256.

Huset, C. A., Barlaz, M. A., Barofsky, D. F., and Field, J. A. (2011). Quantitative determination of fluorochemicals in municipal landfill leachates. *CHEMOSPHERE*, 82(10):1380–1386.

Jahnke, A. and Berger, U. (2009). Trace analysis of per- and polyfluorinated alkyl substances in various matrices-How do current methods perform? *Journal of Chromatography A*, 1216(3):410–421.

Johnson, R. L., Anschutz, A. J., Smolen, J. M., Simcik, M. F., and Penn, R. L. (2007). The adsorption of perfluorooctane sulfonate onto sand, clay, and iron oxide surfaces. *JOURNAL OF CHEMICAL AND ENGINEERING DATA*, 52(4):1165–1170.

Kim, S.-K. and Kannan, K. (2007). Perfluorinated acids in air, rain, snow, surface runoff, and lakes: Relative importance of pathways to contamination of urban lakes. *ENVIRONMENTAL SCIENCE & TECHNOLOGY*, 41(24):8328–8334.

Kwok, K. Y., Taniyasu, S., Yeung, L. W. Y., Murphy, M. B., Lam, P. K. S., Horii, Y., Kannan, K., Petrick, G., Sinha, R. K., and Yamashita, N. (2010). Flux of Perfluorinated Chemicals through Wet Deposition in Japan, the United States, And Several Other Countries. *ENVIRONMENTAL SCIENCE & TECHNOLOGY*, 44(18):7043–7049.

Li, B., Danon-Schaffer, M. N., Li, L. Y., Ikonomou, M. G., and Grace, J. R. (2012). Occurrence of PFCs and PBDEs in Landfill Leachates from Across Canada. *WATER AIR AND SOIL POLLUTION*, 223(6):3365–3372.

Milinovic, J., Lacorte, S., Rigol, A., and Vidal, M. (2016). Sorption of perfluoroalkyl substances in sewage sludge. *ENVIRONMENTAL SCIENCE AND POLLUTION RESEARCH*, 23(9):8339–8348. 1st International Conference on Chemical Biological

Radiological and Nuclear, Research and Innovation (CBRN-RI), Antibes Juan les Pins, FRANCE, MAR 16-18, 2015.

Ochoa-Herrera, V. and Sierra-Alvarez, R. (2008). Removal of perfluorinated surfactants by sorption onto granular activated carbon, zeolite and sludge. *CHEMOSPHERE*, 72(10):1588–1593.

Paul, A. G., Jones, K. C., and Sweetman, A. J. (2009). A First Global Production, Emission, And Environmental Inventory For Perfluorooctane Sulfonate. *ENVIRONMENTAL SCIENCE & TECHNOLOGY*, 43(2):386–392.

Prevedouros, K., Cousins, I., Buck, R., and Korzeniowski, S. (2006). Sources, fate and transport of perfluorocarboxylates. *ENVIRONMENTAL SCIENCE & TECHNOLOGY*, 40(1):32–44.

Rayne, S. and Forest, K. (2009). Perfluoroalkyl sulfonic and carboxylic acids: A critical review of physicochemical properties, levels and patterns in waters and wastewaters, and treatment methods. *JOURNAL OF ENVIRONMENTAL SCIENCE AND HEALTH PART A-TOXIC/HAZARDOUS SUBSTANCES & ENVIRONMENTAL ENGINEERING*, 44(12):1145–1199.

Rhoads, K. R., Janssen, E. M. L., Luthy, R. G., and Criddle, C. S. (2008). Aerobic biotransformation and fate of N-ethyl perfluorooctane sulfonamidoethanol (N-EtFOSE) in activated sludge. *ENVIRONMENTAL SCIENCE & TECHNOLOGY*, 42(8):2873–2878.

Schultz, M. M., Higgins, C. P., Huset, C. A., Luthy, R. G., Barofsky, D. F., and Field, J. A. (2006). Fluorochemical mass flows in a municipal wastewater treatment facility. *ENVIRONMENTAL SCIENCE & TECHNOLOGY*, 40(23):7350–7357.

Sepulvado, J. G., Blaine, A. C., Hundal, L. S., and Higgins, C. P. (2011). Occurrence and Fate of Perfluorochemicals in Soil Following the Land Application of Municipal Biosolids. *ENVIRONMENTAL SCIENCE & TECHNOLOGY*, 45(19):8106–8112.

van Leeuwen, S. P. J. and de Boer, J. (2007). Extraction and clean-up strategies for the analysis of poly- and perfluoroalkyl substances in environmental and human matrices. *JOURNAL OF CHROMATOGRAPHY A*, 1153(1-2):172–185.

van Zelm, R., Huijbregts, M. A. J., Russell, M. H., Jager, T., and van de Meent, D. (2008). MODELING THE ENVIRONMENTAL FATE OF PERFLUOROOCTANOATE AND ITS PRECURSORS FROM GLOBAL FLUOROTELOMER ACRYLATE POLYMER USE. *ENVIRONMENTAL TOXICOLOGY AND CHEMISTRY*, 27(11):2216–2223.

Wang, F., Liu, C., and Shih, K. (2012). Adsorption behavior of perfluorooctanesulfonate (PFOS) and perfluorooctanoate (PFOA) on boehmite. *CHEMOSPHERE*, 89(8):1009–1014.

Wang, F. and Shih, K. (2011). Adsorption of perfluorooctanesulfonate (PFOS) and perfluorooctanoate (PFOA) on alumina: Influence of solution pH and cations. *WATER RESEARCH*, 45(9):2925–2930.

Wang, N., Liu, J., Buck, R. C., Korzeniowski, S. H., Wolstenholme, B. W., Folsom, P. W., and Sulecki, L. M. (2011). 6:2 Fluorotelomer sulfonate aerobic biotransformation in activated sludge of waste water treatment plants. *CHEMOSPHERE*, 82(6):853–858.

Yan, H., Cousins, I. T., Zhang, C., and Zhou, Q. (2015). Perfluoroalkyl acids in municipal landfill leachates from China: Occurrence, fate during leachate treatment and potential impact on groundwater. *SCIENCE OF THE TOTAL ENVIRONMENT*, 524:23–31.

Zhang, S., Lu, X., Wang, N., and Buck, R. C. (2016). Biotransformation potential of 6:2 fluorotelomer sulfonate (6:2 FTSA) in aerobic and anaerobic sediment. *CHEMOSPHERE*, 154:224–230.

6 Appendix

Table 6.1: Flow Points and Modelled Flow Rates

Flow Point	Flow Rate (m^3/d)
F0	4320
F1	4320
F2	4755.92
F3	47520
F4	60681.9401
F5	362650.755
F6	398682.665
F7	580003.183
F8	1028889.22
F9	589879.178
F10	1625527.53
F11	1625527.53

Table 6.2: Information Groundwater Wells

Location	GW-Depth (m)	Well-Depth (m)	Tube Type	Method/Equipment
G10	2.6	4.05	plastic	Akku-Drill pump
G9.1	1.2	8.1	plastic	Battery Pump
G9.2	0.93	8	plastic	Battery Pump
G7	0.87	2.05	Plastic	Akku-Drill Pump
G6	1.6	3	Plastic	Akku-Drill Pump
G8	2.8	4	Plastic	Akku-Drill Pump
G2	1.1	4.78	Plastic	Akku-Drill Pump
G10	0.77	3.1	Plastic	Akku-Drill Pump

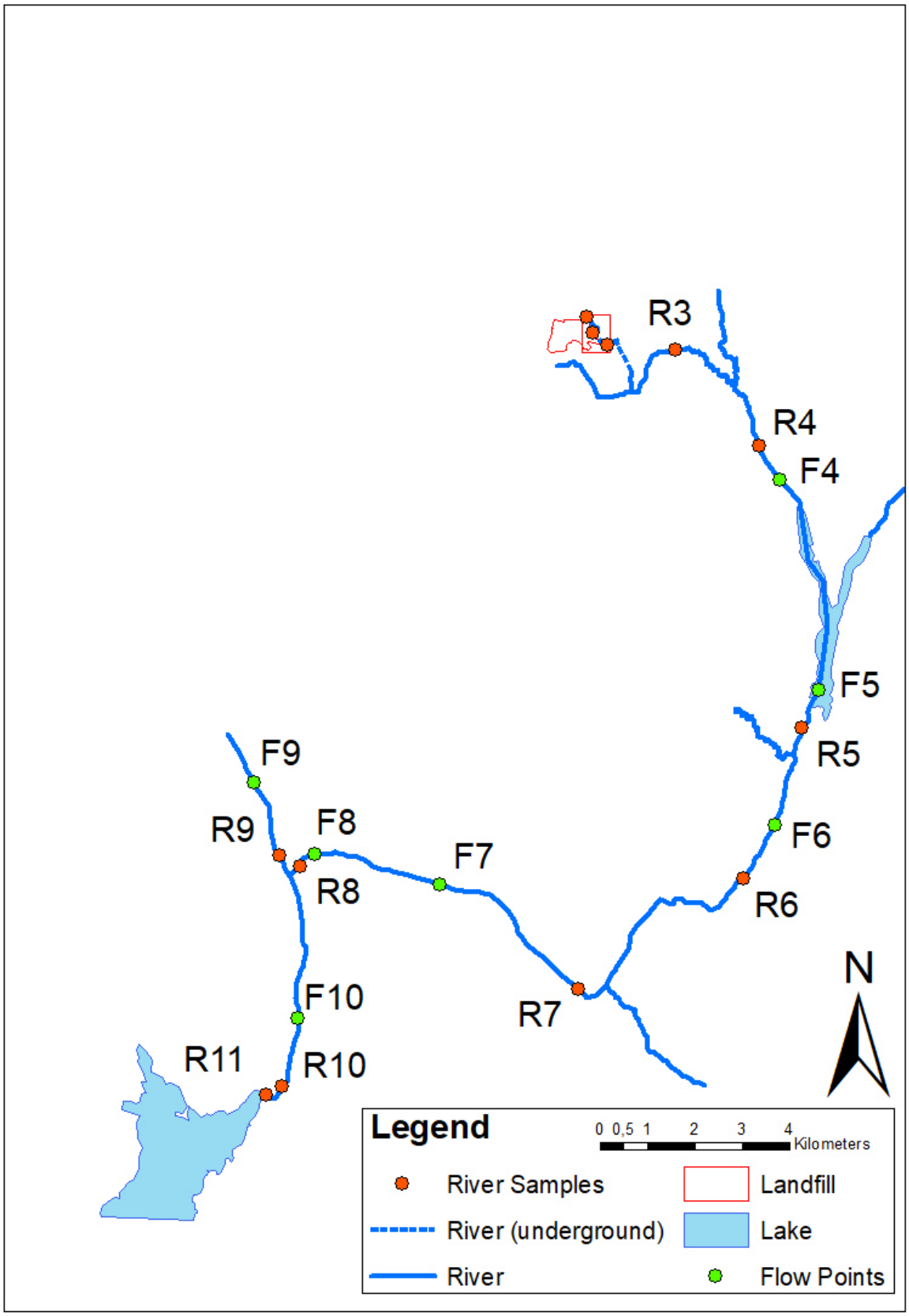

Figure 6.1: Locations of modelled Flow Points